FINITE ELEMENT ANALYSIS OF STRIP FOOTING ON TWO LAYERS OF SAND

Bill V. Stathacopulos

A Dissertation

in

The Faculty

of

Engineering

Presented in Partial Fulfillment of the Requirements
for the degree of Master of Engineering at
Concordia University
Montréal, Québec, Canada

September 1979

ABSTRACT

FINITE-ELEMENT ANALYSIS OF A STRIP FOOTING ON TWO LAYERS OF SAND

Bill V. Stathacopulos

In this investigation the cases of strip footing on a dense sand layer overlying a loose sand deposit and a dense sand layer overlying a compact sand deposit were analyzed theoretically using the finite-element technique. The purpose of this study was to simulate the conditions of the test reported by Hanna, 1978, and to conduct the following studies.

1. To compare the theoretical values of the ultimate bearing capacity obtained from this analysis with the experimental values reported by Hanna (7), and the empirical formulae proposed by Myslivec (19).
2. To predict the upper layer deformation under the footing, and to compare it with the experimental ones reported by Hanna (7).
3. To predict the failure planes of the layers and compare the results with the theoretical ones proposed by Meyerhof and Hanna (14).
4. To plot the pressure bulbs below the strip footing using average pressures taken from 4 elements directly below the footing and discuss the results. Also to compare the soil stress distribution from the finite-element analysis under the footing with the proposed formulae by Boussinesq and the 2:1 stress distribution.

5. To study the behavior of the sand during two dimensional compression by plotting the elastic modulus (E) and shear modulus (G) versus vertical stress.

6. To plot elastic modulus versus the variation of depth of soil and shear modulus in stressed conditions and to compare the curves obtained with the one plotted without any stress applied to the soil.

7. To obtain the horizontal ϵ_h and vertical strain ϵ_v with depth under the footing for an applied stress.

8. To check the validity of the proposed hyperbolic equation, for the non-linear relationship between axial and radial strains during triaxial shear tests, proposed by Kondner and Zelasko (10).

ACKNOWLEDGEMENTS

First, I wish to express my sincere gratitude to Dr.A.M. Hanna, Department of Civil Engineering, Concordia University, for his advice and encouragement he gave me while preparing this work.

I am also grateful to Mr. Tom Davidson and Mr. Jean Jeanmohamed from the Computer Department for their help.

I am thankful to Mr. Ihab Kachef for his advice and to Mr. Steven Duquette who assisted me in drawing the figures.

And also I wish to express my thanks to Christine Filiatrault for typing this report.

TABLE OF CONTENTS

Table of Contents (cont'd)

LIST OF FIGURES

List of Figures (cont'd.)

List of Figures (cont'd.)

LIST OF TABLES

NOTATIONS

a	Reciprocal of the initial tangent modulus
B	Width of footing
b	Reciprocal of the asymptotic value of stress difference
D	Depth of footing
d	Parameter expressing the rate of change of γi with strain
Ei	Initial tangent modulus
Et	Tangent modulus
F	The rate of change of γi with σ_3
f	Value of targent Poisson's ratio at zero strain
G	Value of γi at one atmosphere
K	Modulus number
Nc, Nq, Nγ	Dimensionless bearing capacity factors
n	Exponent
Pa	Atmospheric pressure
q_u	Ultimate bearing capacity per unit area
Rf	Failure ratio
σ_3	Minor principal stress (confining pressure)
$(\sigma_1 - \sigma_3)$	Stress difference
$(\sigma_1 - \sigma_3)f$	Stress difference at failure
$(\sigma_1 - \sigma_3)p$	Stress difference for plane strain
$(\sigma_1 - \sigma_3)t$	Stress difference for triaxial
$(\sigma_1 - \sigma_3)u$	Asymptotic value of stress difference
$\phi^{(1)}$	Angle of internal friction
ϕ_p	Angle of internal friction for plane strain

ϕ_t	Angle of internal friction for triaxial strain
$\gamma^{(2)}$	Unit weight of soil
γ_i	Initial tangent modulus
γ_t	Tangent Poisson's ratio
ε_a	Axial strain
ε_r	Radial strain
ε_v	Volumetric strain

(1) $\phi_1 = 47.7^o$ - Dense sand

ϕ_2 - 35.5^o - Loose sand

or

ϕ_2 - 40.5^o - Compact sand

(2) γ_1 - 104 lbs/ft^3 - Dense sand

γ_2 - 92.64 lbs/ft^3 - Loose sand

γ_2 - 98.3 lbs/ft^3 - Compact sand

CHAPTER I

INTRODUCTION

1.1 General

In foundation engineering two independent aspects must be considered;

1. The ultimate bearing capacity of the soil and
2. The limit of the soil deformation.

The ultimate bearing capacity is the point at which a foundation will fail. Thus, structures can be constructed on a given soil in such a way that the loads of the structures imposed on the soil will not exceed the allowable bearing capacity of that soil. Usually a safety factor of 3 is recommended, Thus

$$q_{all} = \frac{q_{ult}}{3}$$

The limit of the soil deformation determines the load which will cause such deformation of the soil. Thus, the total and differential settlements of the structure should not exceed the limits of the allowable deformation for the stability of the structure. These requirements must be satisfied simultaneously.

The ultimate bearing capacity can be solved by two different approaches:

1. Analytically, by methods such as the theory of plasticity and finite element techniques, or

2. Experimentally, by conducting model and full-scale tests.

Analytical and experimental studies pertaining to the bearing capacity of foundations resting on homogeneous soils are extensive and well documented.

In homogeneous sand deposits the ultimate bearing capacity of a strip footing on sand is a function of the angle of internal friction of the sand as well as the footing width in such a case, the most widely accepted formula for shallow foundations giving the ultimate bearing capacity was developed by Terzaghi using the plasticity theory proposed by Prandtl (1920), and for continuous footings on sand is expressed as:

$$q_{ult} = qN_q + \frac{1}{2}\gamma BN_\gamma \qquad (1)$$

When a footing is placed on stratified deposits, and the thickness of the top stratum is insufficient to fully enclose the rupture zone, then the strength of the lower stratum of the soil will influence the ultimate bearing capacity of this particular soil. It would be expected that the capacity of the soil would increase if the upper soil were stronger and would decrease if it were weaker. In the case of layered soil with different shear strength properties, the soils do not obey the Mohr-Coulomb failure criterion and do not fail simultaneously along a given failure surface, so it is difficult to obtain exact theoritical solutions due to the fact that a suitable stress-strain relationship of the soil must be found. Therefore, an experimental study of such problems would be appropriate

1.2 Purpose and scope of this work

The main objectives of the present work are:

1. To review and discuss the existing bearing capacity theories suggested by various investigators for footings subjected to axial vertical loads and supported on a subsoil having two layers of sand where the upper layer is the stronger.
2. To conduct a theoritical study of the above mentioned case using the finite element technique. The experimental results reported by Hanna (1979) were used for the purpose of comparison.

To achieve the above objectives, a computer program using non-linear finite element analysis was used. And the triaxial test results (Hanna, 1978) were analyzed using the non-linear parabolic relationship proposed by Duncan, 1970.

1.2.1 Thickness of the upper layer

The values of the upper layer thickness used in this investigation are listed below:

$H = 0.5B$

$H = 1.5B$

$H = 2.5B$

$H = 3.5B$ and

$H = 5.0B$

It should be mentioned that for upper layer thicknesses greater than

5B the lower layer has no effect on the ultimate bearing capacity and the design may be based on the bearing capacity of the upper layer of the soil. Where the upper layer can theoretically accommodate a classical failure for uniform soil. It was assumed that the thickness of the lower layer would be such as to simulate the condition of a deep homogeneous thick layer. And the soil below the footing base should have a minimum thickness of 6B for sand, to avoid any boundary effect from the bottom of the experimental box (Meyerhof, 1955).

1.2.2 Shape and size of footing

The analysis was conducted on a surface strip footing having dimensions of width (B) of two inches resting at the center line of the testing box (24"x8"x20")

1.3 Organization of the dissertation

Chapter 2 is a brief literature review of previous work on this subject. A brief description of the equipment, materials, test set-up and procedures used in experimental work is given in Chapter 3. In Chapter 4 an analysis of the triaxial test data and the non-linear stress-strain properties of the sand will be discussed. Chapter 5 will analyse and discuss the finite element results. Finally, in Chapter 6, conclusions will be drawn from the present study and recommendations for future work on this subject given.

CHAPTER 2

REVIEW OF THE PREVIOUS WORK OF TWO LAYERED SOILS

2.1 General

Numerous solutions have been proposed to estimate the bearing capacity of footings on strong layers overlying weak layers. The first proposal was made by Taylor (1948).

The basis of Taylor's solution is that the weak layers such as clays are highly compressible soils. He assumed that the load distribution was 2:1 to the lower layer and considered only its bearing capacity. The problem is conservatively handled. He recognized that this approach was not theoretically accurate, but he indicated that often is was satisfactory.

Button (2) was the first to analyze footings on layered soils of different cohesion but with zero angle of internal friction. With an angle of internal friction = 0^o the curved sector of a d of Fig.2.1 becomes circular. Button actually used a circular segment c a d e with the center above and to the right of point b. The solution was obtained by finding the minimum value of pressure ratio.

$$N_c = \frac{q}{c}$$

where: q = applied footing contact pressure across the width B, and

c = the cohesion of the soil stratum immediately underlying the footing.

Reddy and Srinivasan (1967) extended the Button solution to anisotropic soils defined by a coefficient of anisotropy of the soil immediately underlying the footing as

$$K = \frac{q_1}{q_3}$$

where q_1 = vertical shear strength

q_3 = horizontal shear strength

A value of K<1 indicates over consolidation; K = 1 = isotropic, and K>1 = normally consolidated. Charts from Reddy and Srinivasan are shown for three K values of 0.8, 1.0 and 1.2 in Fig.2.2c. The values for K = 1.0 are identical to those of Button (1953). The bearing capacity for layered soil for conditions Fig.2.2 is given by

$$q_{ult} = c_1 N_c (1 + s'_c + d'_c) + qN_q$$

where: B = width of footing

L = length of footing

$N_q \simeq 1.0$ for $\phi \simeq 0^o$

D = depth of base of footing below ground surface

$s'_c = 0.2B/L$ shape factor

$d'_c = 0.4D/B$ for $D \leq B$

$d'_c = 0.4 \tan^{-1} D/B$ for $D > B$

Desai and Reese (5) applied the finite element technique for footings on layered clay with nonhomogeneity and non-linear stress-strain behavior.

Yamaguchi (1963) considered the layered systems with sand underlain by clay. He employed the same approach as Taylor (1948). and suggested a practical formula.

Based on the experimental results of model loading tests of footings on a subsoil having two layers, Myslivec (19) proposed empirical formulae to calculate the overall bearing capacity. The following cases were considered:

1. Dense sand over loose sand ($\phi_t = 42^o30'$, $\phi_b = 35^o35'$)
2. Loose sand over dense sand ($\phi_t = 35^o35'$, $\phi_b = 42^o30'$)

Clay layers were also considered in Myslivec's analysis. In general, if the bearing capacity of the upper layer was greater than that of the lower one, the lower layer had an effect only when H<B. A higher bearing capacity of the upper layer came into effect only when H>0.2B, then increased linearly with increasing H up to H = B and then after remained constant. If the bearing capacity of the upper layer was smaller than that of the lower layer, the bearing capacity decreased linearly with increasing H up to H>0.7B, then the lower layer had no influence. A summary of the formulae is shown in Fig.2.3

Yves Lebeque (11) after experimentation suggested a simple formula which gives the bearing capacity of a layered sand overlying clay as:

$$q = Kq_o$$

where: q_o is found from the cohesion of clay which is

$$q_o = C(2 + \pi)$$

K is a function of the angle of internal friction of the sand and its relative thickness S/B.

Figs.2.4a and 2.4b give q/q_o as a function of layer thickness over width of foundation.

where: S = depth of upper layer

B = width of footing

C = cohesion of the clay

Several laboratory model studies were attempted by different researchers (Yuan 1957; Narahari and Amarsingh 1964; Brown and Meyerhof 1969; and Rao and Sondhi 1970) to aid in understanding the layer effect on bearing capacity.

Purushothamaraj and Rao (20) investigated the bearing capacity of strip footings in two layered cohesive-friction soils, from which work, solutions have been obtained by the use of Drucker and Proger's (1952) second theorem (kinematic consideration). The N_c values obtained

(for $\phi = 0$ condition) are shown in the Table 1, together with Button's values and Brown and Meyerhof's experimental values. Also in Fig.2.5 the assumed failure mechanism for two layered case is given by Purushothamaraj and Rao.

Table 1. Comparison of N_c values for $\phi = 0$ condition

d/b	Type of analysis	c_2/c_1 = 0.20	0.40	0.80	1.00	1.20	1.60	2.00
	I	2.25	3.05	4.10	4.90	5.45	6.40	7.30
0.25	II	1.90	2.85	4.70	5.52	6.30	7.70	7.70
	III	1.34	2.34	4.30	5.14	5.44	5.82	5.94
	I	3.40	4.20	4.70	4.90	5.00	5.70	5.70
0.50	II	2.55	3.45	4.95	5.52	5.70	5.70	5.70
	III	1.73	2.80	4.60	5.14	5.15	5.41	5.47
	I	4.30	4.75	4.85	4.90	5.00	5.00	5.00
0.75	II	3.20	4.15	5.52	5.52	5.52	5.52	5.52
	III	2.20	3.20	4.93	5.14	5.14	5.14	5.14

Note: I. Limit analysis approach (extrapolated values for $\phi = 0$ condition); II. Button's (1953) limit equilibrium method; and III. Brown and Meyerhof's (1969) experimental values.

For the comparison, values of N_c were obtained by extrapolation. N_c values obtained by this method are somewhat higher than Button's values and Brown and Meyerhof's values for $c_2/c_1<1$ and for $c_2/c_1>1$. The present approach compares well with Brown and Meyerhof's experimental values. Table 2 shows a comparison of bearing capacity values over homogeneous soil conditions.

Table 2. Comparison of bearing capacity values over homogeneous soil condition

		$\phi = 10^o$		$\phi = 20^o$		$\phi = 30^o$		$\phi = 40^o$	
d/b	c_2/c_1	Q	Q'	Q	Q'	Q	Q'	Q	Q'
0.50	0.20	7.0	9.7	33.2	39.4	64.4	82.0	269.0	312.6
	2.00	11.5	9.7	47.0	39.4	102.6	82.0	366.9	312.6
0.75	0.20	8.4	9.7	35.0	39.4	68.3	82.0	273.0	312.6
	2.00	9.7	9.7	43.7	39.4	97.0	82.0	362.0	312.6
1.50	0.20	9.7	9.7	39.4	39.4	77.4	82.0	290.5	312.6
	2.00	9.7	9.7	39.4	39.4	32.0	82.0	329.3	312.6

Note: Q = bearing capacity calculated from charts for layered case: Q' = bearing capacity considering homogeneous case ($c_2 = c_1$).

Meyerhof (16) proposed a theory for the ultimate bearing capacity of a footing punching through a thin sand layer into a thick clay bed. The theory was developed by considering the failure as an inverted uplift problem. Thus at the ultimate load a sand mass having an approximately truncated pyramidal shape is pushed into the clay so that, in the case of general shear failure, the friction angle ϕ and undrained cohesion C of the clay mobilized in the combined failure zones (See Fig.2.6). The approximate ultimate bearing capacity is given by:

$$q_u = cN_c + 2P_p \sin\delta/B + \gamma D \qquad (1)$$

where: $N_c = 5.14$

γ = unit weight of sand

$$P_p = 0.5\gamma H^2(1+2D/H)K_p/\cos\delta \qquad (2)$$

where: K_p = coefficient of passive earth pressure

$\delta = \phi/2$ to $3\phi/4$

In practice it is convenient to use a coefficient K_s so that

$$K_s \tan\phi = K_p \tan\delta \qquad (3)$$

substituting Eqs. 2 and 3 into 1

$$q_u = cN_c + \gamma H^2(1 + 2D/H)K_s \tan\phi/B + \gamma D \qquad (4)$$

with a maximum of:

$$q_u = q_t = \gamma_1 BN_\gamma/2+\gamma DN_q \qquad (5)$$

The punching shear coefficient K_s were given by Meyerhof in Fig.2.7 and Fig.2.8. Fig.2.9 gives typical results of the q_u of model footing tests on dense sand overlying clay.

Meyerhof and Hanna (7) have developed a punching theory for layered soils. They found that the punching shear parameter increases mainly with the bearing capacity ratio q_2/q_1 of the layers, where q_1 and q_2 are the ultimate bearing capacities of strip footing under vertical load on the surfaces of homogeneous thick beds of upper and lower soil, respectively. (Fig.2.10)

CHAPTER 3

EXPERIMENTAL DATA AND TEST PROCEDURE

3.1 General

In foundation problems full scale field tests would be the ideal method to obtain data, but, they are very costly and very difficult in practice, and in turn this restricts the field tests' scope. As an alternative to full scale field tests, carefully conducted model tests can provide useful qualitative and some quantitative data which could be later supplemented with some field tests. The following is a brief discussion of a test procedure for a strip footing model resting on layered soil, as reported by Hanna, (7)

3.2 The model footing

Fig.3.1 shows a model strip footing made from machined aluminum sections. To simulate the rough base of an actual footing, a fine grain sand paper was cemented under the base.

3.3 Model text box

The basic concept in constructing a test box is rigidity so as to avoid any additional strain on the sample due to buckling of the sides of the box. Thick rigid glass was used for the sides so the movement of the soil in the longitudinal direction, due to the applied stress, could be prevented. Fig.3.2 shows the detail construction of the box used for testing.

3.4 Test set-up

A triaxial compression machine is analyzed in this investigation. The work calls for vertical application of stress.

To maintain a vertical direction during the footing test, a loading ram passing through a lubricated ball bearing guide was used. From the above test arrangement, the settlement of the soil of load was recorded incrementally and, by plotting stress versus settlement, the ultimate bearing capacity of the soil was found.

3.5 Soil properties and placing technique

The soil parameters used in the finite element analysis are from the sand described below.

The sand consisted of quartz and feldspar. Grain size distribution is shown in Fig.3.3, and had a uniformity coefficient equal to 2.76.

where: G = 2.64 specific gravity

void ratios and porosities

$e_{max} = 1.010$ $e_{min} = 0.395$

$n_{max} = 0.502$ $n_{min} = 0.283$

Effective size = 0.38mm

Angles of internal friction

Dense sand $\phi_p = 47.7^o$

Compact sand $\phi_p = 40.5^o$, and

Loose sand $\phi_p = 35.5^o$

Dense packing was achieved by raining the sand from a height of 36 inches for each 3-inch layer by means of a metallic sieve; compact packing was achieved by raining the sand from a height of 6 inches for each one inch layer through a funnel with an end sieve; and loose packing was obtained by pouring the sand slowly from one inch height for each one-inch layer, using the same funnel (See Fig.3.4).

CHAPTER 4

TYPICAL EXPERIMENTAL TEST DATA AND STRESS-STRAIN PROPERTIES

4.1 Experimental data

Fig.4.1 shows a footing in two layers of sand. As will be shown in the following discussion, the ratio of H/B was varied to permit study of the effect of the thickness of the upper layer on the ultimate bearing capacity of the soil.

The test results for different combinations of sand follow. At this stage of the test, the deformation of the interface between the two layers was also traced on the glass face of the footing box. Table 4.1a is a summary of the experimental program.

Table 4.1a

Group No.	Type of Footing	Description		Results Table No.
A	strip	D. Sand	Homogeneous Soils	4.2
	strip	L. Sand		
	strip	C. Sand		
B	strip	D. Sand/L.Sand	Strong Layer / Weak Layer	4.3
C	Strip	D. Sand/C.Sand		4.4

4.2 The ultimate bearing capacity

The ultimate bearing capacity is usually determined from load-settlement curves similar in shape to a stress-strain curve. The mode of failure on two layered soil generally depends on the following factors:

1. Size and shape of footing
2. Composition of the supporting coils
3. Character, rate and frequency of the loading
4. Shear strength of upper and lower layers
5. Location of the weaker layer and
6. Finally on the upper layer thickness below the footing base.

Under stress-controlled conditions, footing failure is sudden and catastrophic, and in strain controlled conditions, a visible decrease of load necessary to produce footing movement after a failure may be observed. For practical point of view usually critical settlement is taken as the criterion for failure.

4.3 Typical experimental results

In this section typical experimental results of loading tests on footing are illustrated by load-settlement curves.

Based on observations of footing tests, the following are summarized. For footings in a strong layer overlying a weak layer under vertical loads, the load settlement curves were found to possess

a peak value at higher H/B ratios where the mode of failure was general shear. The degree of curvature of the load settlement curves decreased with a decrease of the H/B ratio, while the mode of failure changed to local shear failure.

Table 4.2

Group A

Test results: Footings in homogeneous soils

Type of Footing	Type of Soil	Test No.	Footing Depth D / Footing Width B	Ultimate Load q_u (psi)	Settlement at Failure (S/B)%
Strip	D. Sand ϕ = 47.7	1	0.0	34.32	9.0
Strip	L. Sand ϕ = 34.0	7	0.0	2.60	30.0
Strip	C. Sand ϕ = 42.4	13	0.0	11.15	14.5

Table 4.3

Group B

Test results: Strip footing in dense sand* overlying loose sand**

Series No.	Test No.	$\frac{H}{B}$	Ultimate Load q_u (psi)	Settlement At Failure (S/B)%	Footing Location
1	17	0.25	2.93	30.0	surface
	18	0.5	3.69	28.0	
	19	1.0	5.32	26.0	
	20	2.0	10.55	24.5	
	21	3.0	17.54	21.5	
	22	4.5	33.61	17.0	
	23	5.0	34.50	16.0	

* $\phi_1 = 47.7^\circ$ ** $\phi_2 = 34.0^\circ$

Table 4.4

Group C

Test results: Strip footing on dense sand* overlying compact sand**

Test No.	$\frac{H}{B}$	$\frac{h}{B}$	Ultimate Load q_u (psi)	Settlement at Failure (S/B)%
36	0.5	0.5	16.12	14.0
37	1.0	1.0	22.67	13.0
38	1.5	1.5	30.48	12.0
30	2.0	2.0	33.95	11.5

* $\phi_1 = 47.7^\circ$ ** $\phi_2 = 42.4^\circ$

CHAPTER 5

THE FINITE ELEMENT ANALYSIS

5.1 General

Before the development of electronic computers, it was not feasible to perform analyses of stresses in soil masses for other than assumed linear elastic soil behavior. Now, however, due to the availability of high-speed computers and powerful numerical analytical techniques such as the finite element method, it is possible to approximate non-linear inelastic soil behavior in stress analyses.

In this method, the soil mass is assumed to consist of a finite number of discrete elements interconnected at a finite number of nodal points. The properties of the elements are adjusted so that the assemblage of elements behaves in the same manner as the original continuum.

5.2 Geometry of the continuum

Hrennikoff (8), McHenry (15), and McCormick (12) have discussed the use of finite-element analysis, using a lattice analogy to represent the continuum.

Clough (4) and Wilson (24) have done extensive work with the finite element technique.

The analysis in finite element theory (in this investigation) is done by assuming the continuum to be divided into elements.

These elements are interconnected at nodal points, and a stiffness matrix equation relating the forces and the deflections at the nodal points is developed. Three conditions must be satisfied in the theory of finite-element analysis in order to develop the stiffness matrix equation:

1. The deformations of adjacent elements must be compatible
2. The forces acting on the element must be in equilibrium; and
3. The displacements of each element as a result of the applied forces must be consistent with the physical properties of the material.

5.3 Steps in the finite-element analysis

The finite-element analysis consists of the following basic operations:

1. Development of a stiffness matrix of an arbitrary element with respect to a convenient local coordinate system.
2. Development of a transformation matrix (constraint matrix) to transform the stiffness matrix from the local coordinate system to a generalized coordinate system.
3. Generation of the final stiffness matrix for the entire assemblage, incorporating the boundary forces, body forces and deflections.
4. Solution of the system of simultaneous equations, which can be represented by a block tridiagonal matrix equation. A recursive method has been employed in this work to solve the simultaneous equations.

5.4 Data given to be used in the finite-element analysis

The following data are given by Hanna (1978).

1. Loose silica sand

$\phi = 35.5^{o}$ (Angle of internal friction)

$n = 43.8\%$ (Porosity)

$e = 0.779$ (Void ratio)

$\gamma = 92.64 lbs/ft^3$ (Unit weight of sand)

$G = 2.64$ (Specific gravity)

where: $\gamma = \frac{G}{1+e}\gamma_w = \frac{2.64}{1+0.779} \times 62.43 = 92.64 \text{ lbs/ft}^3$

$e = \frac{n}{1-n} = \frac{.438}{1-0.438} = 0.779$

2. Compact silica sand

$\phi = 40.5^{o}$

$n = 40.4\%$

$e = 0.677$

$\gamma \doteq 98.3 \text{ lbs/ft}^3$

$G = 2.64$

3. Dense silica sand

$\phi = 47.7^{o}$

$n = 36.9\%$

$e = 0.584$

$\gamma = 104$ lbs/ft^3

Other data for this sand are:

$e_{max} = 1.01$ $\quad$ $e_{min} = 0.395$

$n_{max} = 50.2\%$ $\quad$ $n_{min} = 28.3\%$

and $(\sigma_1 - \sigma_3)$ versus axial strain curves for loose, compact and dense sand with σ_3 are given in Appendix I.

5.5 Finite-element analysis

The computer program used herein was developed by Kulhawy et al (9). This analysis employs non-linear, stress-dependent, stress-strain relationships for the tangent modulus and the tangent Poisson's ratio of the enbankment soils. The tangent modulus variation is expressed by the hyperbolic relationship proposed by Kondner and Zelasko (10). The tangent Poisson's ratio variation is developed in a similar manner and is based upon a hyperbolic equation.

The program is composed of one principal program LSBUILD and six sub-routines (LAYOUT, LSSTIF, LSQUAD, LST8, BANSOL and LSRESL). See Appendix II for user guide to the program.

The main characteristic in developing this program was the use of non-linear analysis of stress-strain of the triaxial test data utilizing Kondner's (10) theory, and also a simplified practical non-linear stress-strain relationship used by Duncan and Chang (6) in finite element analysis.

5.6 Non linear stress analysis

In order to perform non linear stress analysis in soils it is necessary to be able to describe the stress-strain behavior of soil in quantitative terms, and to develop techniques for incorporating this behavior in the analyses.

A simplified, practical non linear stress-strain relationship which is convenient to use with the finite element method of analysis is described herein. The parameters which describe this relationship are ϕ, K, n, Rf, G, F, d. One parameter involved in this relationship is ϕ which is the Mohr-Coulomb strength parameter. The remaining parameters involved in the proposed relationship can be evaluated using the triaxial stress-strain curves of the same test used to determine the value of ϕ.

5.6.1. Non linearity and stress-dependency

Kodner and Zelasko (1962) have shown that the non linear stress-strain curves of both clay and sand may be approximated by hyperbolae. The hyperbolic equation proposed by Kodner was:

$$(\sigma_1 - \sigma_3) = \frac{\varepsilon}{a + b\varepsilon}$$

where: σ_1 and σ_3 = the major and minor principal stresses

ε = The axial strain, and

a and b = constants whose values may be determined experimentaly.

The physical meaning of the constants a and b can be seen in Fig. 5.1a

By plotting stress-strain data (in the form shown above) it is easy to determine the values of the parameters a and b. The following pages show the detail procedure how the parameters are found. It may be noted (in Figs. 5.3a to 5.3c) that data diverge somewhat from linear relationship at both low and high values of strain, indicating that the stress-strain curve for the test is <u>not</u> precisely hyperbolic in shape.

1. Convert the angle of internal friction ϕ from triaxial to plane-strain using Fig. 5.1b

See tables 5.1.a to 5.1.f. for different values of ϕ.

2. Convert given data from triaxial to plane-strain. (See Tables 5.1.a, 5.1.b etc...).

Example: Take, for example, Table 5.1.f for $(\sigma_1 - \sigma_3)_t = 28.5$psi. This value is read from the stress-strain curves from a standard triaxial test, in the same curve the value of $\varepsilon_t = 4.0$ is also read.

$$\sin\phi = \frac{(\sigma_1 - \sigma_3)}{(\sigma_1 + \sigma_3)} = \frac{(28.5)}{(10 + 38.5)} = 0.5876$$

$$\phi_t = \arcsin(0.5876) = 35.99$$

for $\phi_t = 35.99^o$ go to Fig.5.1 and find $\phi_p = 38.0^o$

then $\sin\phi_p = 0.6156$

but $\sin\phi_p = \dfrac{(\sigma_1 - \sigma_3)_p}{(\sigma_1 + \sigma_3)_p}$ $\quad (\sigma_3)_t = 10\text{psi}$

therefore $0.6156 = \dfrac{(\sigma_1 - 10)}{(\sigma_1 + 10)}$, solving we get $(\sigma_1)_p = 42.03$

which gives us $(\sigma_1 - \sigma_3)_p = 32.03$ $\quad \varepsilon_t/(\sigma_1 - \sigma_3)_p$ 0.001249

The remaining values are found in similar manner.

3. Transform the stress-strain curve for the given sand. In Figs.5.2a to 5.2c the parameters E_i and $(\sigma_1 - \sigma_3)_{ult}$ are found. To find the above mentioned parameters, Fig.5.2 of axial strain/stress difference $(\varepsilon_a/(\sigma_1 - \sigma_3)$ is plotted for each type of sand. A straight line is fitted through the points, and the slope of this line (b) and the lower intercept of the line at zero axial strain is found. Then $E_i = 1/a$ and $(\sigma_1 - \sigma_3)_{ult} = 1/b$ values are found. These appear on every graph for each case of σ_3 (See Figs.5.2b and 5.2c).

DENSE SILICA SAND

Fig. 5.1.a, 5.1.b, 5.1.c, and 5.1.d.

$\phi = 47.7^{o}$ (Initial)

n = 36.9%

Table. 5.1.a - CONVERTING DATA FROM TRIAXIAL TO PLANE STRAIN

$(\sigma_1 - \sigma_3)_t$	ε_t%	ϕ_t	ϕ_p	sin ϕ_p	$(\sigma_1 - \sigma_3)_p$	$e/(\sigma_1 - \sigma_3)_p$	σ_3
90	.6	22.02	25.14	.4248	110.78	0.005416	75
105	.7	24.31	27.76	.4657	130.74	0.005354	"
130	.9	27.6	31.52	.5228	164.33	0.005476	"
172	1.4	32.3	36.9	.6004	225.37	0.006212	"
205	2.0	35.27	40.3	.6467	274.57	0.007284	"
233	2.9	37.47	42.8	.6794	317.87	0.009123	"
243	3.4	38.2	43.62	.6898	333.6	0.010192	"
260	4.6	39.35	44.93	.7062	360.6	0.01275	"
266	5.7	39.74	45.38	.7117	370.3	0.01539	"
267	6.9	39.81	45.46	.7127	372.1	0.01854	"
260	8.6	39.35	44.93	.7062	360.55	0.02385	"
253	9.7	38.88	44.4	.6996	349.33	0.02776	"
243	10.8	38.2	43.62	.6898	333.56	0.03237	"
235	12.0	37.6	42.93	.6811	320.36	0.03745	"

Table 5.1.b - CONVERTING DATA FROM TRIAXIAL TO PLANE STRAIN

$(\sigma_1 \quad \sigma_3)_t$	ϵ_t%	ϕ_t	ϕ_p	sin ϕ_p	$(\sigma_1 - \sigma_3)_p$	$\epsilon/(\sigma_1 - \sigma_3)_p$	σ_3
35	0.2	17.72	20.23	.3457	42.27	0.00473	40
47	0.3	21.72	24.8	.4194	57.8	0.00519	"
65	0.5	26.63	30.41	.5062	82.	0.0061	"
85	0.8	31.	35.4	.5793	110.2	0.00726	"
110	1.3	35.37	40.4	.6481	147.33	0.0088	"
120	1.5	36.86	42.09	.6703	162.64	0.00922	"
130	1.8	38.24	43.67	.6905	178.5	0.01008	"
135	2.1	38.9	44.42	.6999	186.58	0.01125	"
145	2.7	40.12	45.82	.7171	202.8	0.0133	"
155	3.8	41.26	47.12	.7328	219.4	0.0173	"
158	4.9	41.6	47.5	.7372	224.4	0.0218	"
157	6.0	41.48	47.3	.7349	222.78	0.02705	"
153	6.4	41	46.82	.7292	215.4	0.0297	"
145	8.4	40.12	45.6	.7145	200.21	0.0419	"

Table 5.1.c - CONVERTING DATA FROM TRIAXIAL TO PLANE STRAIN

$(\sigma_1 - \sigma_3)_t$	ε_t%	ϕ_t	ϕ_p	sin ϕ_p	$(\sigma_1 - \sigma_3)_p$	$\varepsilon/(\sigma_1 - \sigma_3)_p$	σ_3
15	0.4	25.4	29	.4848	18.82	0.02125	10
21	0.6	30.8	35.17	.576	27.17	0.02208	"
26	0.8	34.42	39.31	.6335	34.57	0.02324	"
32	1.0	37.98	43.37	.6867	43.83	0.02281	"
37	1.4	40.5	46.25	.7224	52.05	0.02689	"
41	1.8	42.23	48.22	.7457	58.65	0.03069	"
45	2.4	43.81	50	.766	65.47	0.03665	"
48	3.2	44.9	51.27	.78	70.91	0.04512	"
48	3.6	44.9	51.27	.78	70.91	0.05076	"
46	4.9	44.2	50.47	.7713	67.45	0.07264	"
45	6.0	43.8	50	.766	65.47	0.09164	"
43	7.0	43	49	.7558	61.9	0.11308	"

Table 5.1.d - CONVERTING DATA FROM TRIAXIAL TO PLANE STRAIN

$(\sigma_1 - \sigma_3)_t$	ϵ_t%	ϕ_t	ϕ_p	sin ϕ_p	$(\sigma_1 - \sigma_3)_p$	$\epsilon/(\sigma_1 - \sigma_3)_p$	$\dot{\sigma}_3$
5	0.2	22.62	25.83	.4357	6.17	0.0324	4
10	0.4	33.74	38.53	.6229	13.21	0.03028	"
12	0.6	36.87	42.1	.6704	16.27	0.03687	"
14	0.8	39.52	45.13	.7087	19.46	0.0411	"
16	1.0	41.8	47.73	.74	22.77	0.043917	"
17	1.2	42.8	48.87	.7532	24.41	0.04916	"
19	1.4	44.72	51.1	.7782	28.06	0.04989	"
20	1.8	45.6	52.1	.789	29.91	0.06018	"
21	2.2	46.4	52.98	.7984	31.7	0.0694	"
20	3.4	45.6	52.07	.7887	29.86	0.11386	"

COMPACT SILICA SAND

$\phi = 40.5^{o}$ (Initial)

n = 41.2%

Table 5.1.e - CONVERTING DATA FROM TRIAXIAL TO PLANE STRAIN

$(\sigma_1 - \sigma_3)_t$	ε_t%	ϕ_t	ϕ_p	sin ϕ_p	$(\sigma_1 - \sigma_3)_p$	$\varepsilon / (\sigma_1 - \sigma_3)_p$	σ_3
17.5	.4	27.8	27.8	.4663	17.5	0.000228	10
18	.6	28.3	28.3	.4740	18.0	0.000333	"
28	1.0	35.7	36.8	.5990	29.9	0.00334	"
35.5	2.0	39.7	43.6	.6896	44.4	0.00045	"
37	2.5	40.5	44.3	.6984	46.3	0.00054	"
38	3.0	40.9	45	.7071	48.3	0.00062	"
38.5	4.0	41.1	45.2	.7095	48.8	0.00082	"
37	5.0	40.5	44.3	.6984	44.4	0.00112	"
35.5	6.0	39.7	43.6	.6896	44.43	0.00135	"
35	7.0	39.5	43.2	.6845	43.4	0.0016	"
34.5	8.0	39.2	42.9	.6807	42.6	0.00187	"
34	9.0	39	42.5	.6755	41.6	0.00216	"
33	10	38.5	41.9	.6678	40.2	0.00248	"
32.5	11	38.2	41.0	.6560	38.1	0.00288	"
32	12	37.9	40.7	.6520	37.5	0.0032	10

LOOSE SILICA SAND

ϕ = 35.5° (Initial)

n = 43.8%

Table 5.1.f - CONVERTING DATA FROM TRIAXIAL TO PLANE STRAIN

$(\sigma_1 - \sigma_3)_t$	ε_t%	ϕ_t	ϕ_p	$\sin \phi_p$	$(\sigma_1 - \sigma_3)_p$	$\varepsilon/(\sigma_1 - \sigma_3)_p$	σ_3
5	.2	11.53	11.53	.1998	5	0.0004	10
8.5	.4	17.35	17.35	.2982	8.5	0.00047	"
16	.6	26.38	26.38	.4443	16.	0.000375	"
21	1.0	30.81	30.81	.5122	21.	0.000476	"
25	1.8	33.75	34.5	.5664	26.12	0.000689	"
27	2.7	35.06	37.0	.6018	30.22	0.000893	"
28.5	4.0	35.99	38.0	.6156	32.03	0.001249	"
29.2	5.7	36.40	38.3	.6197	32.59	0.00175	"
29.2	7.3	36.40	38.3	.6197	32.59	0.00223	"
29.4	9.3	36.52	39.0	.6293	33.95	0.00274	"
29.4	11.0	36.52	39.0	.6293	33.95	0.00324	10

5.6.2. Stress-dependency

Except inthe case of unconsolidated undrained saturated soils, both the tangent modulus and the compressive strenght of soils have been found to vary with the contining pressure employed in test. Experimental studies by Jambu (1968) have shown that the relationship between initial tangent modulus and confining pressure may be expressed as:

$$Ei = K\ Pa\ \left(\frac{\sigma_3}{Pa}\right)^n$$

where: Ei = initial tangent modulus

σ_3 = minor principal stress

Pa = atmospheric pressure

K = a modulus number

n = the exponent determining the rate of variation of Ei with σ_3.

To find K, n a graph was plotted using Ei versus confining pressure (σ_3). A straight line was fitted through the points. K is read from the lower interception of this line at one psi and n is the slope of the line. See Fig. 5.4 for values of K and n. The values obtained from Fig. 5.4 are as follows:

For dense sand:

K = 2429

n = 0.543

$$n = \frac{\text{Log } 10{,}000 - \text{Log } 6{,}000}{\text{Log } 27 - \text{Log } 5} = 0.543$$

For compact sand:

$K = 1450$

$n = 0.5776$ $\quad n = \frac{\text{Log } 10{,}000 - \text{Log } 4{,}000}{\text{Log } 25 - \text{Log } 4.5} = 0.5776$ and

For loose sand:

$K = 700$

$n = 0.653$ $\quad n = \frac{\text{Log } 9{,}000 - \text{Log } 2{,}000}{\text{Log } 40 - \text{Log } 4} = 0.653$

The asymptotic value may be related to the compressive strength by means of a factor R_f as shown by:

$$(\sigma_1 - \sigma_3)_f = R_f (\sigma_1 - \sigma_3)_{ult}$$

Therefore:

For dense sand:

$R_f = 1$ (using Fig.5.2a and Table 5.1a)

For compact sand:

Example given

$$R_f = \frac{(\sigma_1 - \sigma_3)_t}{(\sigma_1 - \sigma_3)_{ult}} = \frac{38.5}{42.7} = 0.901$$

For loose sand:

$R_f = 0.905$

5.6.3. Procedures for nonlinear stress analyses.

Nonlinear, stress-dependent stress-strain behavior may be approximated in finite analyses by assigning different modulus values to each of the elements into which the soil is subdivided for purposes of analysis as shown in Fig. 5.1c The modulus value assigned to each element is selected on the basis of the stresses or strains in each element. Because the modulus values depend on the stresses and the stresses in turn depend on the modulus values, it is necessary to make repeated analysis to insure that the modulus values and the stress conditions correspond for each element in the system.

Two techniques for approximate nonlinear stress analysis are shown in Fig. 5.3.

In the present investigation the iterative procedure is used, shown on the left-hand side of Fig. 5.3, in this method the same change in external loading is analyzed repeatedly. After each analysis, the values of stress and strain within each element are examined to determine if they satisfy the appropriate nonlinear relationship between stress and strain. If the values of stress and strain do not correspond, a new value of modulus is selected for that element for the next analysis.

The principal advantage of the iterative procedure is the fact that it is possible, by means of this procedure, to represent stress-strain relationships in which the stress decreases with increasing strain after reaching a peak value. The shortcoming of the iterative procedure is that it is very difficult to take into account nonzero initial stresses.

5.6.4. Tangent modulus values

If the value of the minor principal stress is constant, the tangent modulus, E_t may be expressed as:

$$E_t = \frac{\partial(\sigma_1-\sigma_3)}{\partial\varepsilon}$$

It should be pointed out that the stress-strain relationship described has been derived on the basis of data obtained from standard triaxial tests in which the intermediate principal stress is equal to the minor principal stress, because in most practical cases only triaxial test data are available. However, this same relationship may be used for plane strain problems in which the intermediate principal stress is not equal to the minor principal stress, if appropriate plane strain test results are available.

5.6.5 Tangent Poisson's ratio

Values of Poisson's ratio for dense sand generally increase with the stress level on primary loading, as would be expected for dense sand which dilates (expands) under large shear stresses.

Values of Poisson's ratio for loose sand vary somewhat less with stress level. This phenomenon was observed from test results. It is evident from the above discussion that it is not possible to characterize the behavior of the sand accurately by a single value of Poisson's ratio. Moreover, because the sand dilates under the action of shear stresses, the most appropriate stress-strain relationship would reflect the influence of shear stresses on volume changes. Kulhawy, Duncan and Seed (9) demonstrated that hyperbolic equation can be used to describe the non-linear relationship between the axial and radial strains during triaxial shear tests in the form of:

$$\frac{\varepsilon_r}{\varepsilon_a} = f + d\varepsilon_r$$

where: ε_r = the radial strain

ε_a = axial strain

f = the value of tangent Poisson's ratio at zero strain or the initial tangent Poisson's ratio, γ_i;

d = the parameter expressing the rate of change of γ_i with strain.

The values of γ_i and d can be determined by plotting the values of $\varepsilon_r/\varepsilon_a$ against ε_r and fitting a straight line as shown in Fig.5.5. The value of γ_i is the intercept of this line with zero radial strain (ε_r) and d is the slope of this line.

7. Find the parameters G and F (Poisson's ratio parameters)

The value of γ_i was found to vary semilogarithmically in the form of:

$$\gamma_i = G - F\log\frac{\sigma_3}{Pa}$$

where: G = the value of γ_i at one atmosphere;

F = the rate of change of γ_i with σ_3; and

Pa = atmospheric pressure in the same units as σ_3

The values of G and F can be determined from the results of a series of triaxial tests by plotting the values of γ_i against $\frac{\sigma_3}{Pa}$ on a semi-logscale and fitting a straight line the obtained data is shown in Fig.5.6. The example given is for dense sand. After a straight line is fitted through the points a vertical line from $(\sigma_3/Pa) = 1.0$ is drawn until it intercepts the line for dense sand, then a horizontal line is drawn and the value of G is read from the vertical scale. (See also Fig.5.6).

It should be noted that:

$$\varepsilon_r = \frac{\varepsilon_v - \varepsilon_a}{2}$$

where: $\varepsilon_v = \Delta v/v$

The G and F values to be used in this study, were taken from Duncan and Chang (6) for the loose sand and, for the compact sand, interpolated due to the lack of sufficient experimental data.

Table 5.6

Obtained values of stress-strain parameters

for the finite element analysis

PARAMETERS	Values Employed in Analyses		
	DENSE SAND	COMPACT SAND	LOOSE SAND
Unit weight, γ, in pounds, per cubic foot	104	98.3	92.64
Friction angle, ϕ, in 0^{o}	47.7	40.5	35.5
Modulus number, K	2429.	1450.	700
Modulus exponent, n	0.543	0.577	0.653
Failure ratio, R_f	1.0	0.901	0.905
Poisson's ratio parameters			
G	0.4010	0.485	0.431
F	0.1140	0.103	0.087
d	13.8	4.28	2.5

5.7 Finite element computer results and analysis

The finite element program used in this analysis was developed by Kulhawy, F.H., and Duncah, J.M., (9). This program calculates the stresses and strains in a Dam section under its own weight, for this reason the incremental application of the load on the footing had to be simulated as layers of soil with very high density.

The finite element model (Mesh) is shown in Fig.5.1c The mesh is 24" wide and 20" high. The strip footing 2" wide by 6" high rests on the surface of the layered sand. The entire mesh contains 120 elements and 148 nodal points, from 1 to 108 elements with from 1 to 130 nodal points constitute the layered sand, and from 109 to 120 elements with 123 to 148 nodal points simulates the footing. It can be seen from Fig.5.1c that all the nodal points along the vertical boundaries and along the bottom horizontal boundary of the layered sand are fixed, while the rest are unrestrained.

To simulate applied stresses, the six layers of the footing are given a value of γ at each iteration equal to the stress increment required and are divided by the volume of the layer. As an example, if a stress increment of one (1) Psi is required on the first iteration, then P will be equal to 2.0 Psi, and, in effect, the applied load will be (1 x 144) (2) = 288 lbs - linear foot, on 144 lbs/ft^2 - linear foot.

The load increments are chosen in such a manner that the computer will search at least 5 layers. This is equal to 10 iterations (2 iterations per layer are used for accuracy) before the ultimate capacity of the soil is reached.

is reached. The tables 5.7a and 5.7b give the results of the finite-element analysis from the different layer combinations used.

Table 5.7a

Group A'

Finite element results: Strip footing in Dense sand* overlying Loose sand**

Iterations per Layer	Test No.	H/B	Ultimate Load q_u (psi)	Settlement at Failure (S/B)%	Footing Location
2	1	0.5	4.7	11.2(1)	SURFACE FOOTING
	2	1.5	6.81	7.0	
	3	2.5	17.6	7.0	
	4	3.5	26.5	8.0	
	5	5.0	33.	7.5	

* $\phi_1 = 47.7^0$ ** $\phi_2 = 35.5^0$

Table 5.7b

Group B'

Finite element results: Strip footing in Dense sand*

overlying Compact sand***

Iterations per Layer	Test No.	$\frac{H}{B}$	Ultimate Load q_u (psi)	Settlement at Failure (S/B)%	Footing Location
2	6	0.5	14.0	11.5(2)	SURFACE FOOTING
	7	1.5	26.0	9.5	
	8	2.5	33.5	7.0	
	9	3.5	33.5	7.0	
	10	5.0	34.5	8.0	

*** $\phi_2 = 40.5$

5.8 Discussion of the finite element obtained results.

Figs.5.7 and 5.8 are plots of pressure versus settlement/width of footing, and Figs.5.9 and 5.10 show the ultimate bearing capacity q_u versus the ratio H/B for surface strip footing on dense sand overlying loose sand, and dense sand overlying compact sand respectively. For comparison, the experimental test results of Hanna (7) are also plotted in these Figs. It is necessary to discuss briefly here how the finite-element obtained results for settlement were plotted. As an example the case of H/B = 3.5 for dense/compact sand will be explained. From the computer out-put for dense/compact sand with H/B = 3.5 we get:

$q^{(1)}$ (psi)	settlement$^{(2)}$ (inch)
9	- 0.0170
19.39	- 0.0662
25.34	- 0.1428
37.98	- 0.2821
37.98	- 0.2931
37.98	- 0.3048

(1) The q is taken as the average value of elements 101, 102, 103 and 104. (See Fig.5.1c)

(2) The settlement is that of the node number 124.

This combination of sand layers fails at 33.5 psi (See Table 5.7b). It is interesting to observe in the finite-element obtained results that beyond 37.9 psi there is practically no settlement. It can also be seen

that inspite the continuing incremental application of stress on the soil no stress increase was recorded on the finite-elements 101, 102, 103 and 104 above 37.9 psi. This suggests that the soil reached the peak value of strain and after that the stress decreases or remains constant (according to the iterative procedure) . The stagnation of the settlement value can also be attributed to the same fact (no more stress increase).

In real life situation additional settlement of the sand can be observed only if much higher stresses will be applied on the soil and the sand particles begin to crush. But before this begins in a footing when the critical value of stress is reached, the footing will develop differential settlement and simply colapses sideways in a clearly defined failure plane.

Fig.5.11 shows the local angle of shearing resistance (failure plane) for a strip footing resting on a strong layer of sand overlying a weak layer of sand. Fig.5.12 shows the layer settlement under a strip footing in dense sand overlying loose sand. The experimental results in this Fig. were taken from a time exposure picture (Hanna 1978) and were plotted along with the analytical results for comparison.

Fig.5.13 shows the pressure isobars below a strip footing. Fig.5.13 cannot be compared with Boussinesq because Boussinesq's results are only for one layer soil (homogeneous soil).

It is interesting to note in Fig.5.13 that the pressure bulb is interrupted at the interface of the two different soils and continues to form a different bulb with lower values than the upper layer. Also, in the lower layer there is a region of low pressure (0.24) independent of the other pressure regions.

Fig.5.14 shows the behavior of the sand during two dimensional compression and how elastic modulus (E) and shear modulus (G) vary with applied stress. This is expected because the value of E is given by:

$$E = \frac{\sigma}{\varepsilon}$$ and the value of G by $$G = \frac{E}{2(1 - \nu)} = \frac{\tau_{xy}}{\gamma_{xy}}$$

Fig.5.15 shows the variation of elastic modulus (E) and shear modulus (G) with depth.

Finally, Fig.5.16 shows the average horizontal strain (ε_h) and vertical strain (ε_v) and how they differ with depth.

5.9 Homogeneous Soils

In homogeneous soils the stresses in a soil mass due to footing pressure can be computed using several proposed methods the most widely used is the 2:1 and Boussinesq's method. For the 2:1 method the applied pressure on the soil is assumed to be distributed in a slope of 2:1

The change in pressure Δq at a depth z beneath the footing is given by: (See Fig. 5.17)

$$\Delta q = \frac{V}{(B + z)(L + z)} \qquad (1a)$$

where: V = total load applied to foundation member

B, L = footing dimensions

z = depth from footing base to elevation in soil, where increase in stress is desired.

For a depth z = 4.5 in, V = 18 lbs, B = 2" and L = 1" we get using formula 1a.

$$\Delta q = \frac{18}{(2 + 4.5)(1 + 4.5)} = 0.363$$

therefore: $\Delta q = 0.363$ theory

$\Delta q = 0.08$ Boussinesq(1)

$\Delta q = 0.474$ finite-element

(1) Boussinesq values are for point load and are taken from Bowles(1)

The immediate settlement for homogeneous soils such as non-saturated clays and silts, sands and gravels both saturated and unsaturated can be computed from the following equation:

$$S_1 = qB \frac{1 - \mu^2}{E_s} I_w$$

where: S = settlement

q = intensity of contact pressure

B = least lateral dimension of footing

I_w = influence factor which depends on shape of footing and its rigidity.

E_s, μ = elastic properties of soil

As an example for a soil with E_s = 7,000 psi, μ = 0.25, q = 37.98 psi, I_w = 5.06 and B = 2" (all the above values were taken from Bowles 1977). Using the above formula the settlement can be computed as:

$$S_1 = 37.98(2)\frac{1 - (0.25)^2}{7000}(5.06) = 0.0514 \text{ in}$$

S_1 = 0.0514 from theory, and

** S_2 = 0.2821 from finite-element

** In Fig.5.10 it was shown that for dense/compact soil in H/B >2 the soil behaved as homogeneous. If we take the settlement results obtained from the finite-element analysis for H/B = 3.5 in same sand these results are for homogeneous soil and can be compared with the above mentioned formula. So we have for q = 37.98 S_2 = 0.2821

For lower stresses say q = 11.5 psi we get:

S_1 = 0.01558 and

S_2 = 0.0170

It can be seen that only for low stresses the settlement (S_1) from the theoretical formula agrees with the settlement (S_2) results obtained using the finite-element method.

CHAPTER 6

CONCLUSION AND RECOMMENDATIONS

6.1 Strong layer overlying weak layer

The important conclusions drawn from the analysis of previous theories and experimental results, plus the investigation of the present work, are summarized as follows.

It can be seen from Figs. 5.9 and 5.10 that the obtained results, from finite element analysis, compare very well with the experimental results reported by Hanna (7) (within 5%). Thus the punching theory proposed by Hanna is considered to be an acceptable tool in evaluating the bearing capacity of layered soils.

The empirical formulae proposed by Myslivec do not agree with the present investigation. Myslivec has proposed that when the upper layer thickness H is equal B then the lower layer has not effect on the bearing capacity of the soil, but the present analytical investigation as well as Hanna's experimental work have shown that this is not true. (see Figs' 2.3, 5.9 and 5.10).

The large discrepancy of the settlement values obtained from the experimental values reported by Hanna, as it can be seen in Fig.5.7 and 5.8, to that of the finite-element method, is attributed to the strain controlled conditions of the test and the finite-element which is stress controlled.

In homogeneous case the theoretical settlement formula gives very low values for stresses near the ultimate bearing capacity of the soil. By comparing the obtained results of the finite-element analysis with the reported results of other researchers (Duncan and Chang, 6, Chiyyarath and Reese, 3, using tests, it is concluded that the finite-element obtained results are close to what might be expected in a real case.

The distribution of the local angle of shearing resistance on the failure plane found in finite-element analysis compares well with the theoretical failure plane proposed by Meyerhof and Hanna (14) for two layered soil.

The pressure bulb obtained from this investigation in two layered soil cannot be compared because there is not similar study in existence. But in the homogeneous case the change of pressure obtained using 2:1 formula gives relatively close values to the one found using the finite-element analysis, while values obtained by the Boussinesq method are very low in comparison with both the 2:1 and finite-element method.

The elastic modulus (E) and shear modulus (G) increase with increasing stress. Also the elastic and shear moduluses vary with depth (See Fig.5.15) and increase with applied stress but the increase is non-linear.

The vertical strain (ε_1) and horizontal strain (ε_3) have a discontinuity at the interface of the two different soil. In homogeneous soils there is always a smooth transition of the strain intensity through out the soil.

The consistency of the obtained results in this investigation suggests that the proposed by Kondner and Zelasko (10) hyperbolic stress-strain relation in sands is a valid assumption.

Analyses of the results obtained by previous researchers using theory and tests, plus the results of the present investigation revealed that the factors that determine the ultimate bearing capacity of a strip footing in a strong layer overlying a weak layer are the following:

1. The shear strength of the upper and lower layers.
2. The relative strength of the upper and lower layers.
3. Thickness of the upper layer below footing base (H).
4. Depth of the footing in the upper layer, D.
   (In this investigation D ≐ 0)
5. Shape of footing
6. Compressibilities of component layers
7. Water table

6.2 Recommendations

The results obtained by the finite element method suggests that the method can be applied in other combinations of layered soil such as clay-sand and silts-sand, and the lower layer can also be Rock. More than two layered soils can also be investigated using the same method with predicting good results.

6.3 Limitations of the finite element method

The following are the limitations of this method:

1. Cannot predict accurately settlements.
2. A computer is required to perform the calculations. It must also be noted here that the User of this program requires a high field length (1577B or in that order) and a high time limit (T1000).
3. The parameters to be used in this method must be available or else should be found using tests.
4. The value of the incremental stress which is applied on the soil through the footing must be chosen accordingly.

END

FIGURES

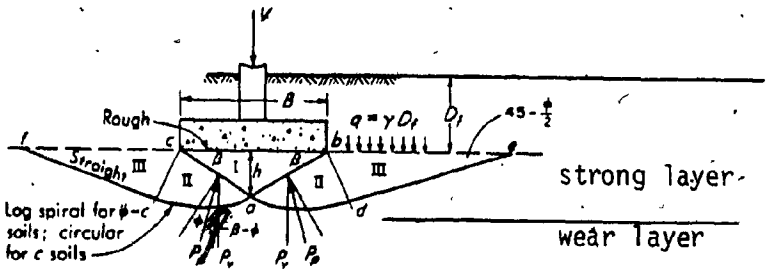

Fig.2.1 Button failure planes

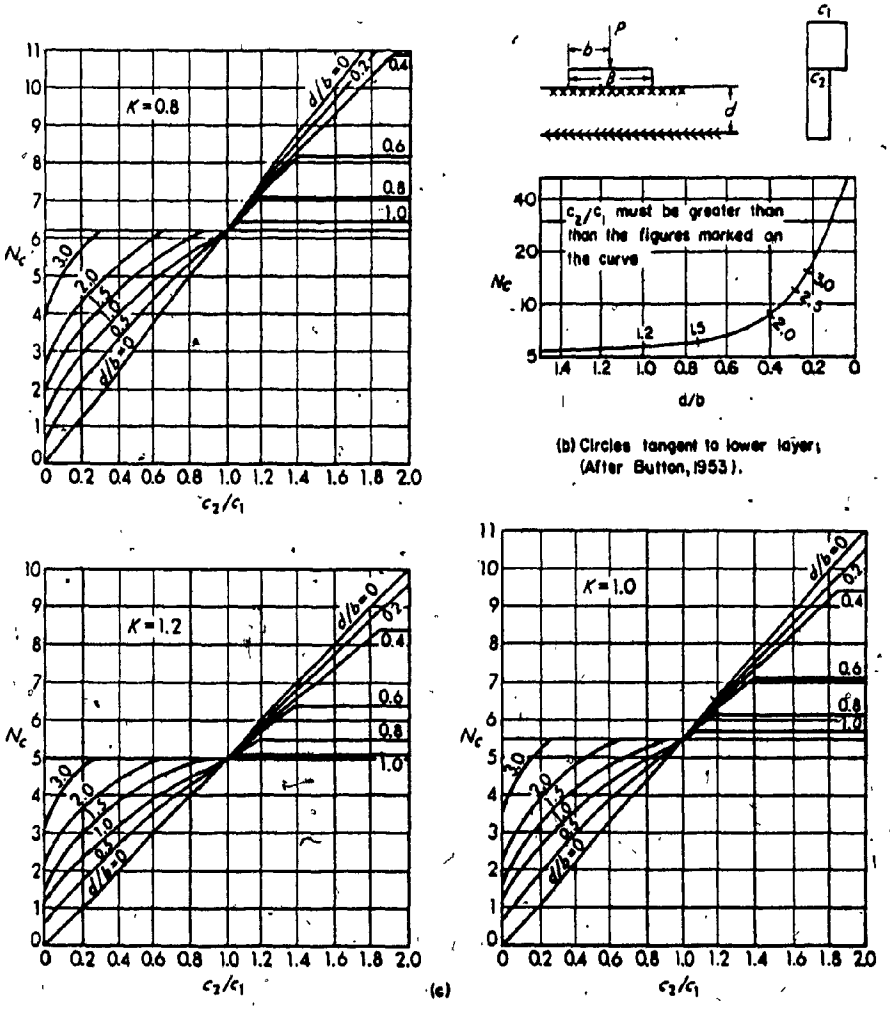

Fig.2.2 Bearing-capacity factors for a footing located on a two-layer cohesive soil system, with cohesion in each layer as shown. (After Reddy and Srinivasan (21))

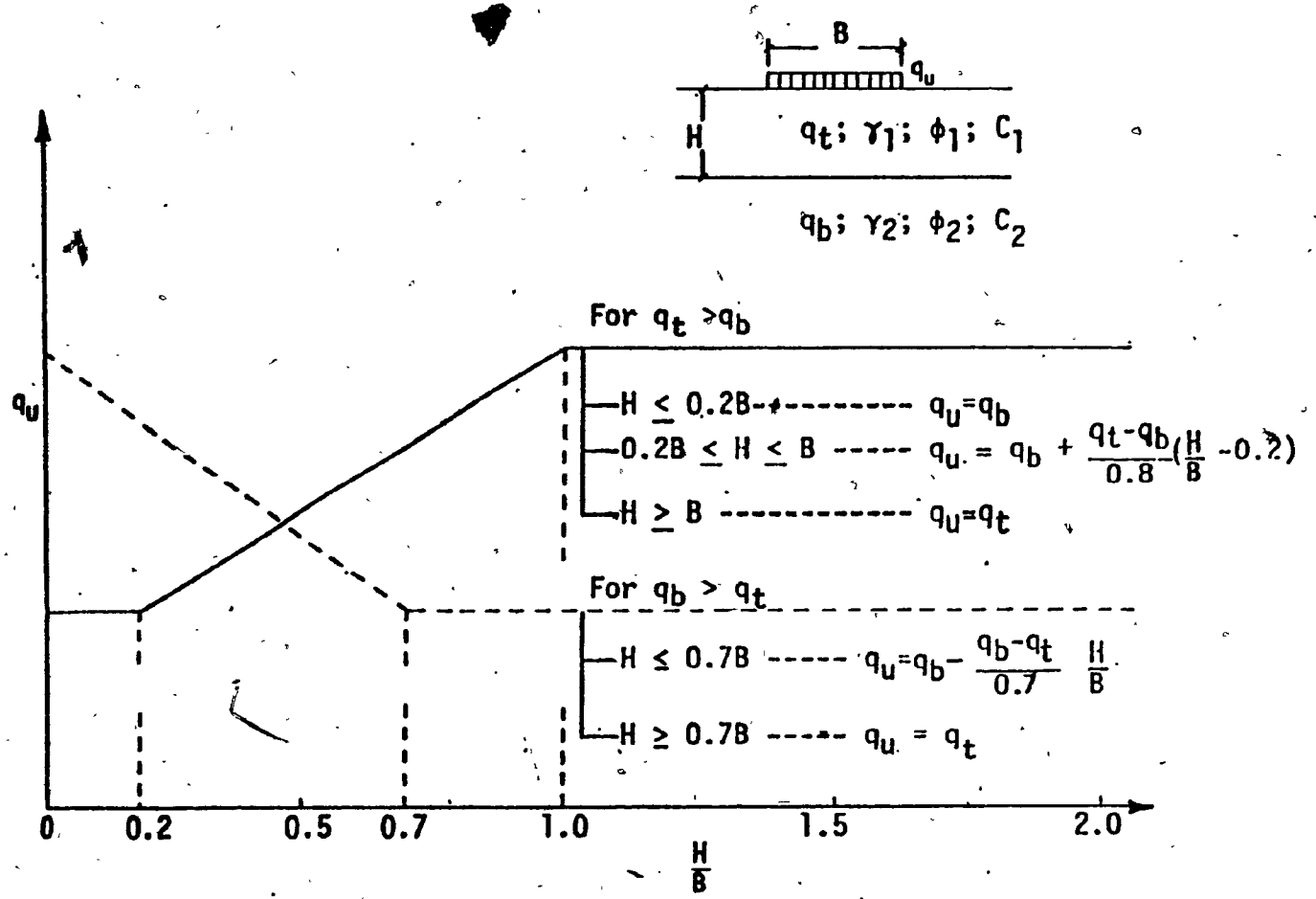

Fig.2.3 Myslivec's analysis.

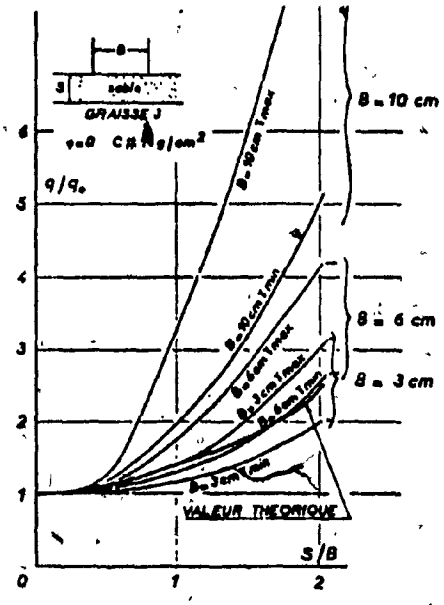

Fig.2.4a The value of q/q_0 is given as function of the sand thickness for a clay with high C factor. (After Lebeque)

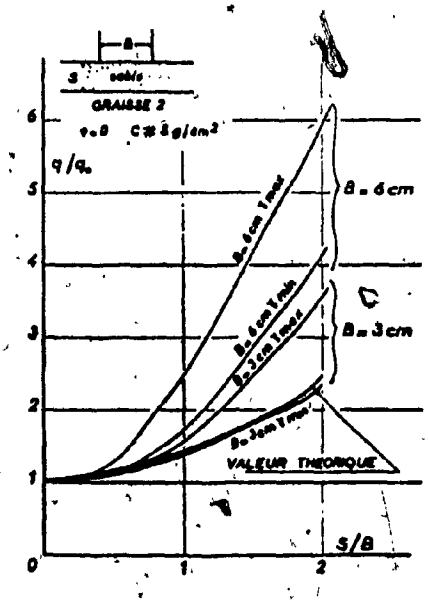

Fig.2.4b The value of q/q_0 is given as a function of the sand thickness for a clay with low cohesion factor C.

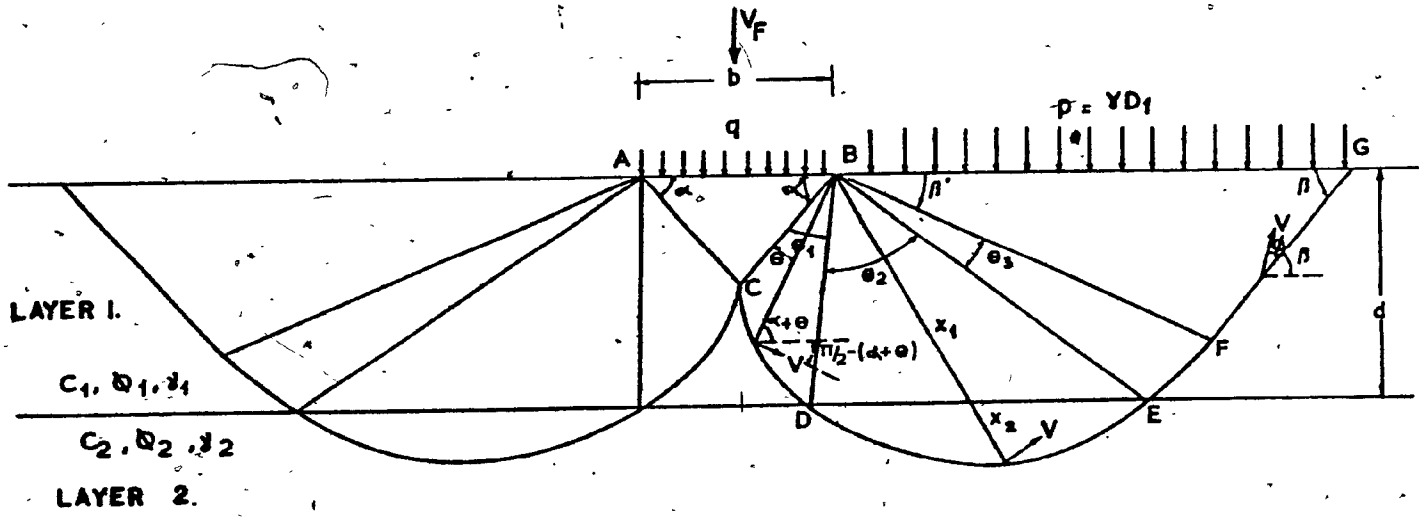

Fig.2.5 Assumed failure mechanism for two layered case, used by Purushothamaraj and Rao in their analysis.

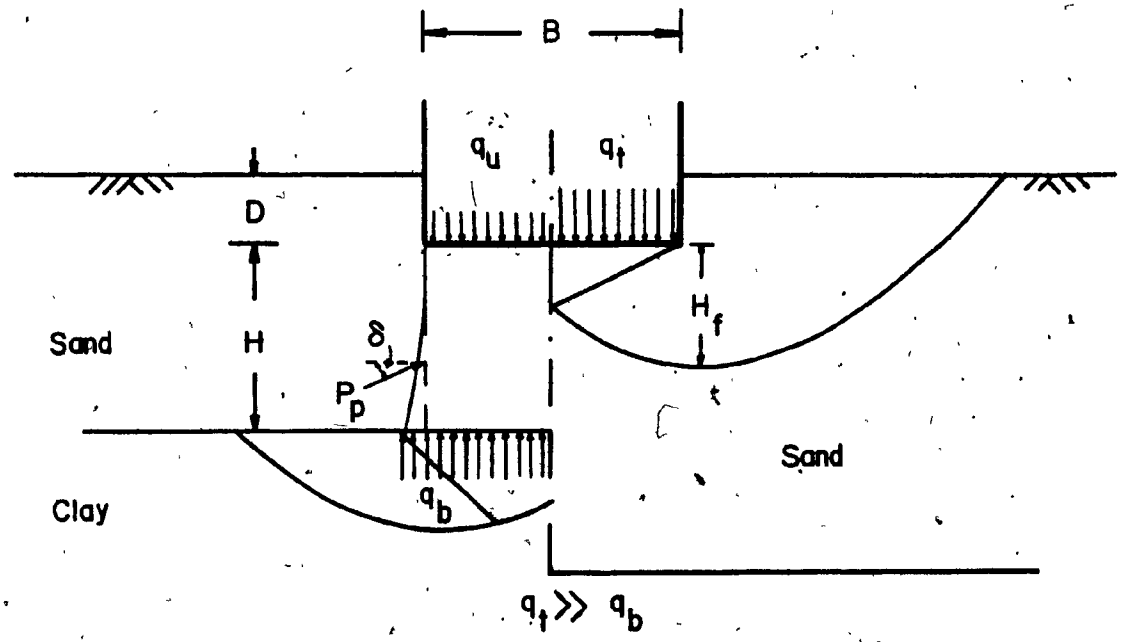

(a) THIN LAYER (b) THICK LAYER

FIG. 2.6 FAILURE OF SOIL BELOW FOOTING ON DENSE SAND LAYER ABOVE SOFT CLAY.
(After Meyerhof, (16))

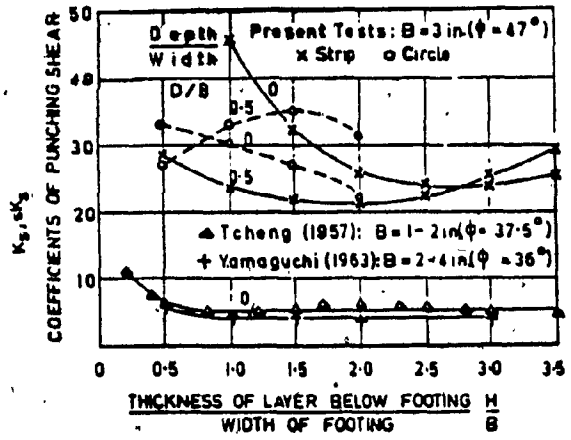

Fig.2.8 Experimental punching shear coefficients for model tests. (After Meyerhof ,(16).)

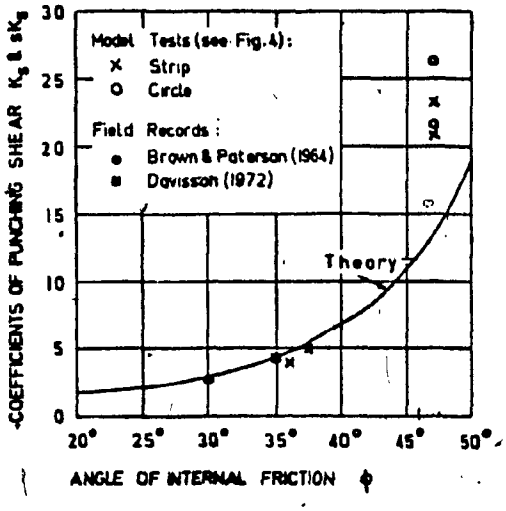

Fig.2.7 Coefficients of punching shearing resistance.

(Both Figs. After Meyerhof,(16))

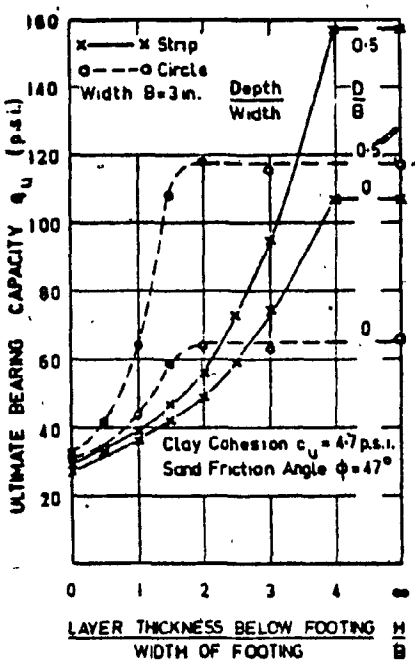

Fig.2.9 Typical results of model footing tests on dense sand overlying clay.

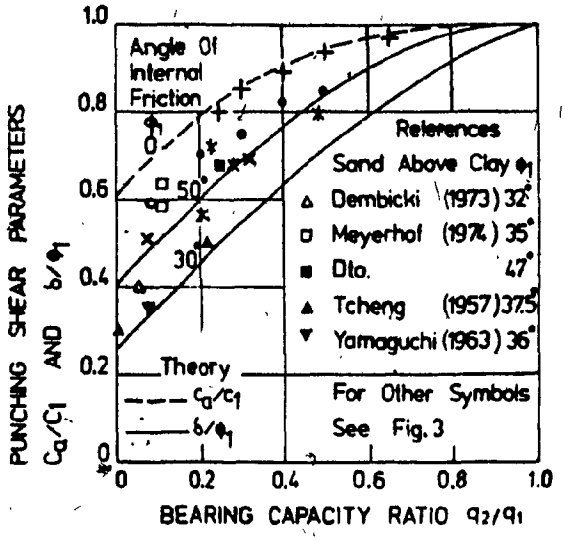

Fig.2.10 Punching shear parameters under vertical load. (After Meyerhof (16)).

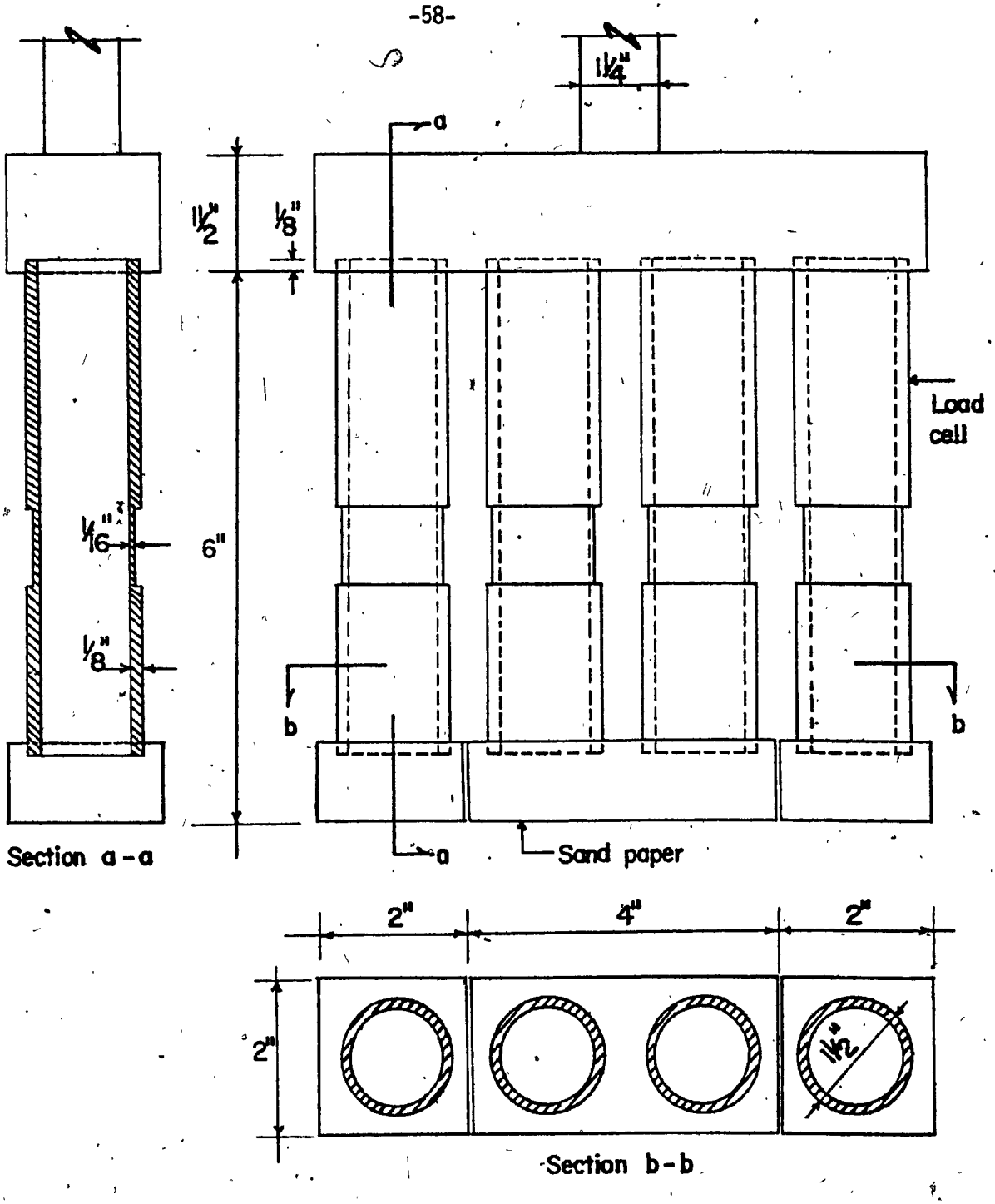

FIGURE 3.1 MODEL STRIP FOOTING - FOR VERTICAL LOADS (THREE PIECE FOOTING)

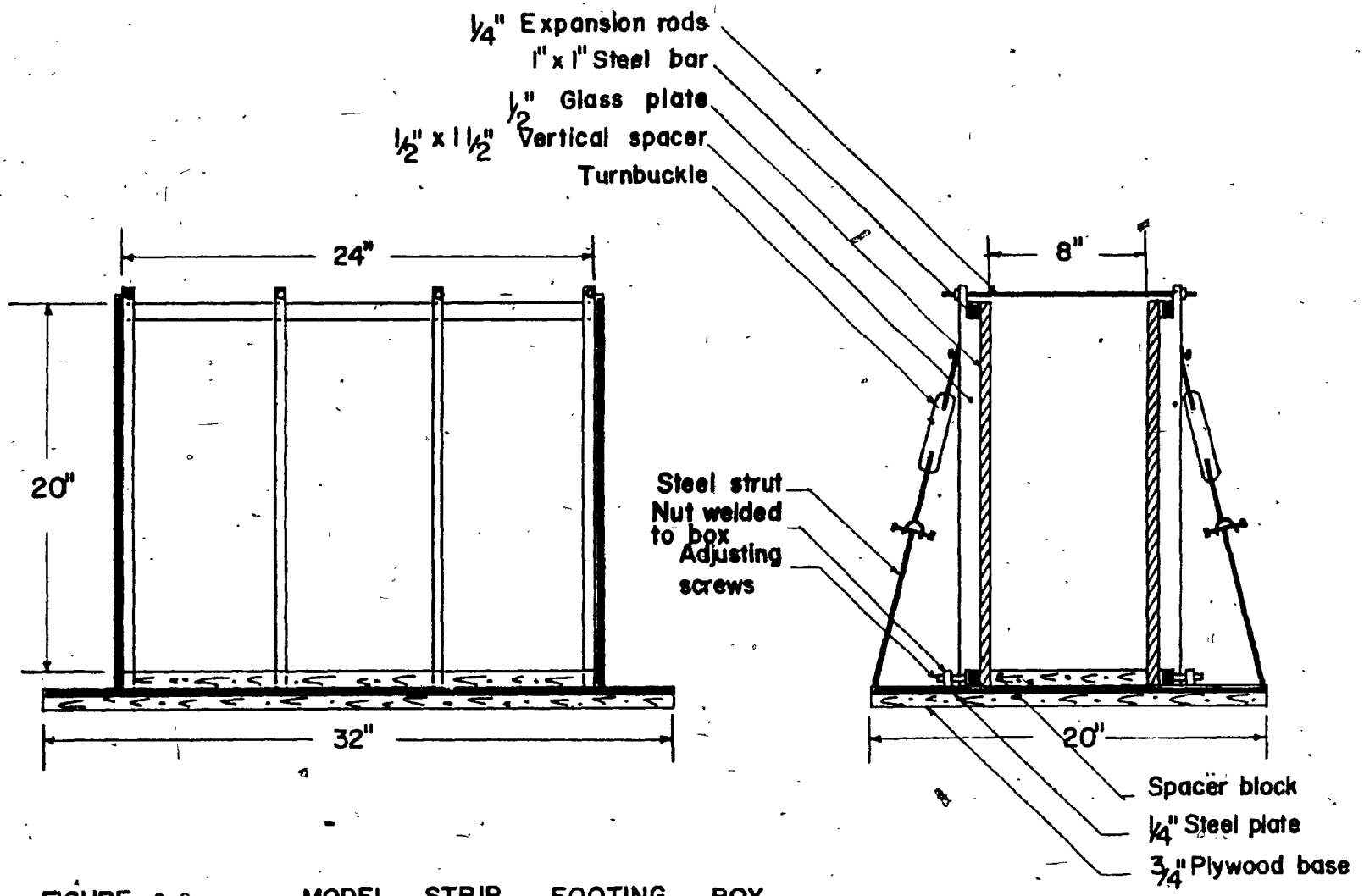

FIGURE 3.2 MODEL STRIP FOOTING BOX

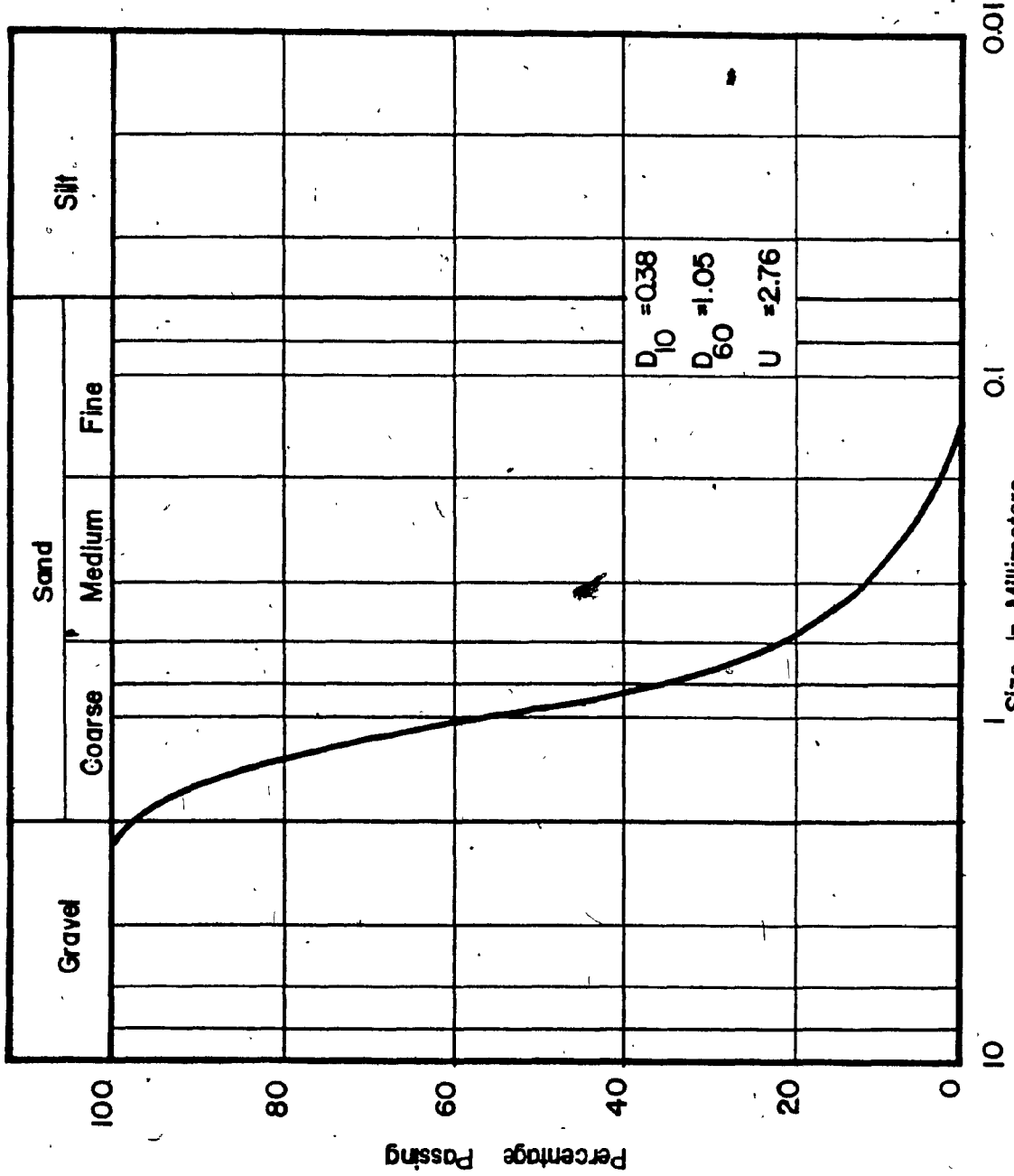

FIGURE 3.3 GRAIN SIZE DISTRIBUTION OF THE SAND.

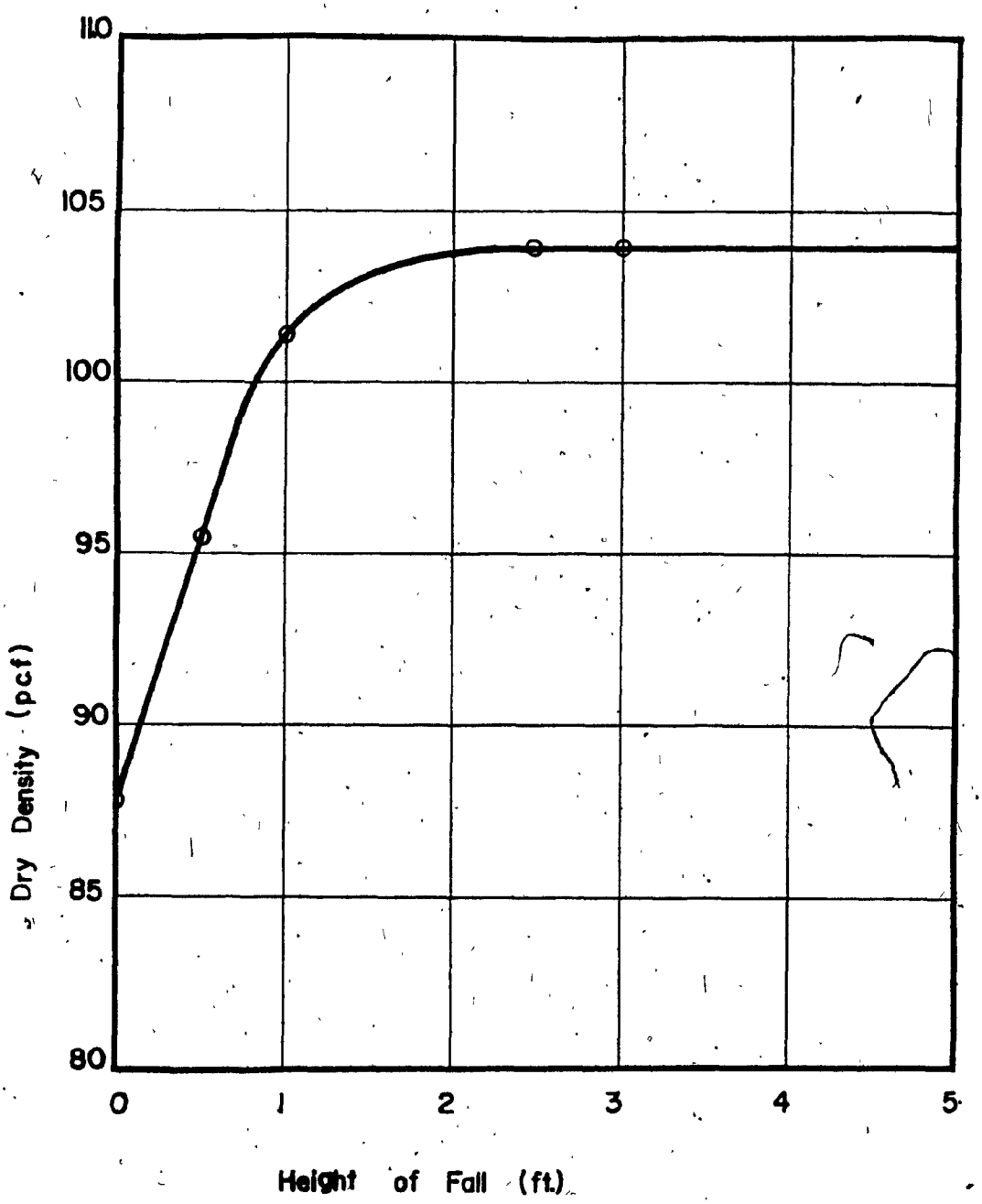

FIGURE 3.4 RELATIONSHIP BETWEEN SAND DENSITY AND HEIGHT OF FALL

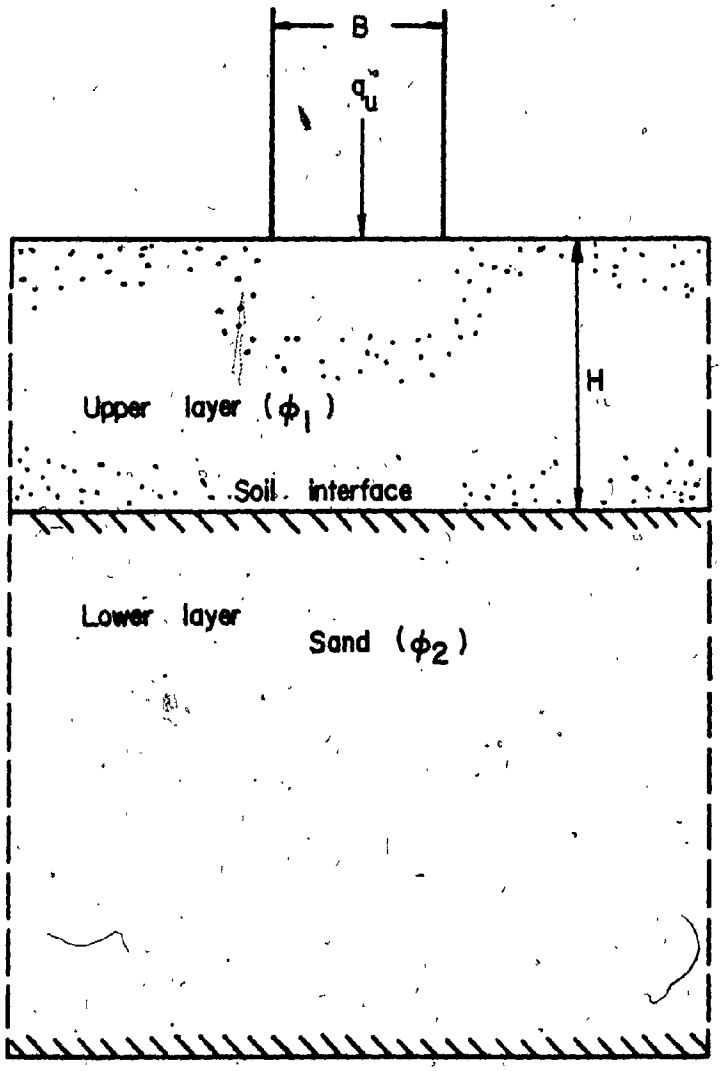

FIG. 4.1 FOOTING IN A TWO LAYERED SOIL

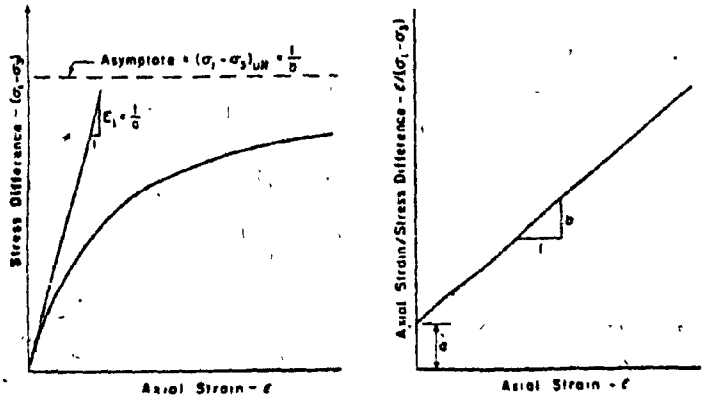

Fig.5.1a Hyperbolic stress-strain curve and Transformed hyperbolic stress-strain curve.

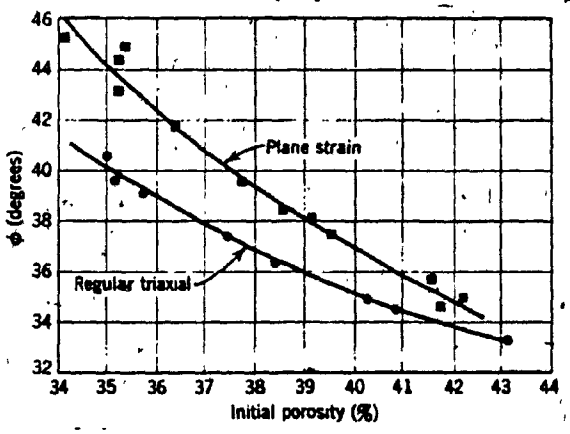

Fig.5.1b Results of regular and plane-strain triaxial tests (After Cornforth).

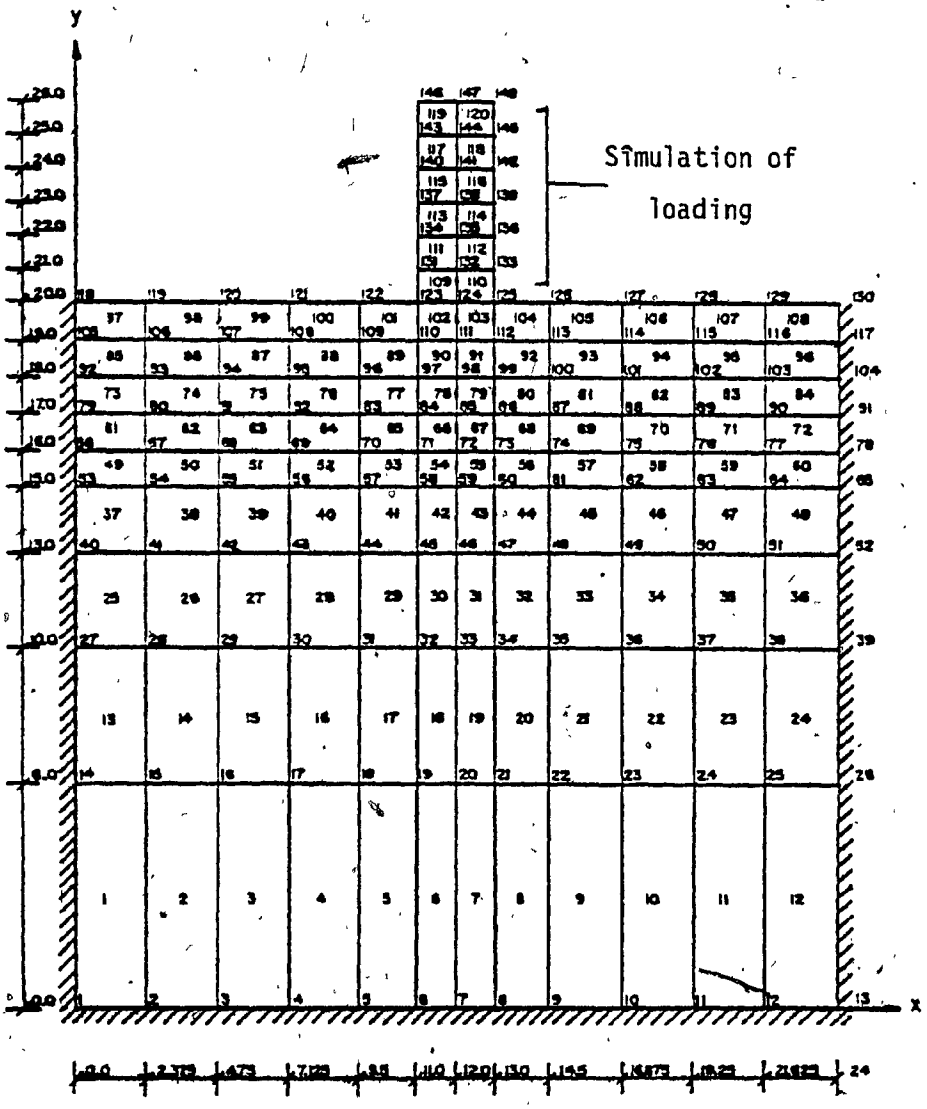

FIG. 5-1 C[illegible]INITE ELEMENT MODEL OF THE SUPPORTING SOIL AND SIMULATION OF FOUNDATION LOAD

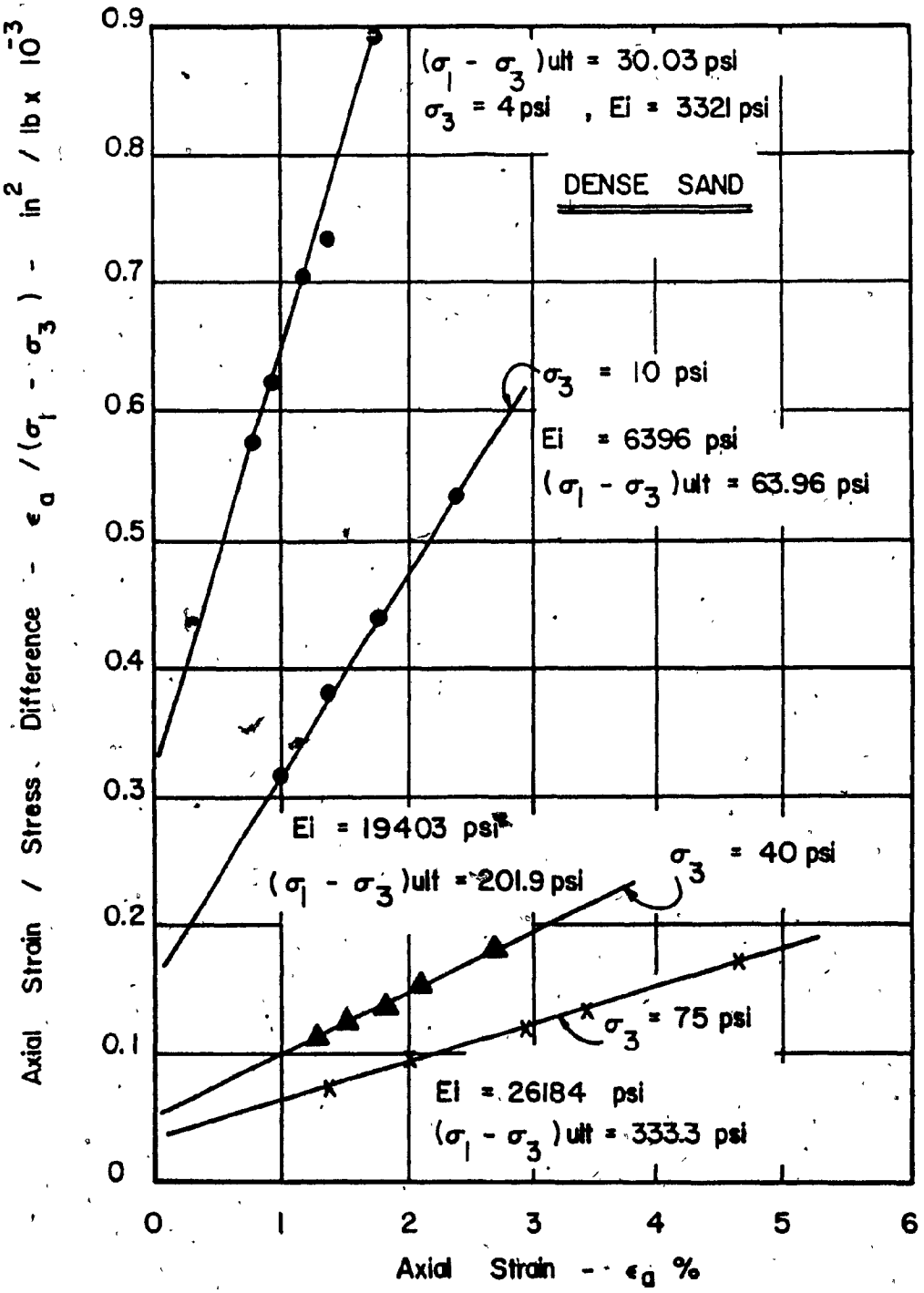

FIG. 5.2 a TRANSFORMED STRESS - STRAIN CURVE

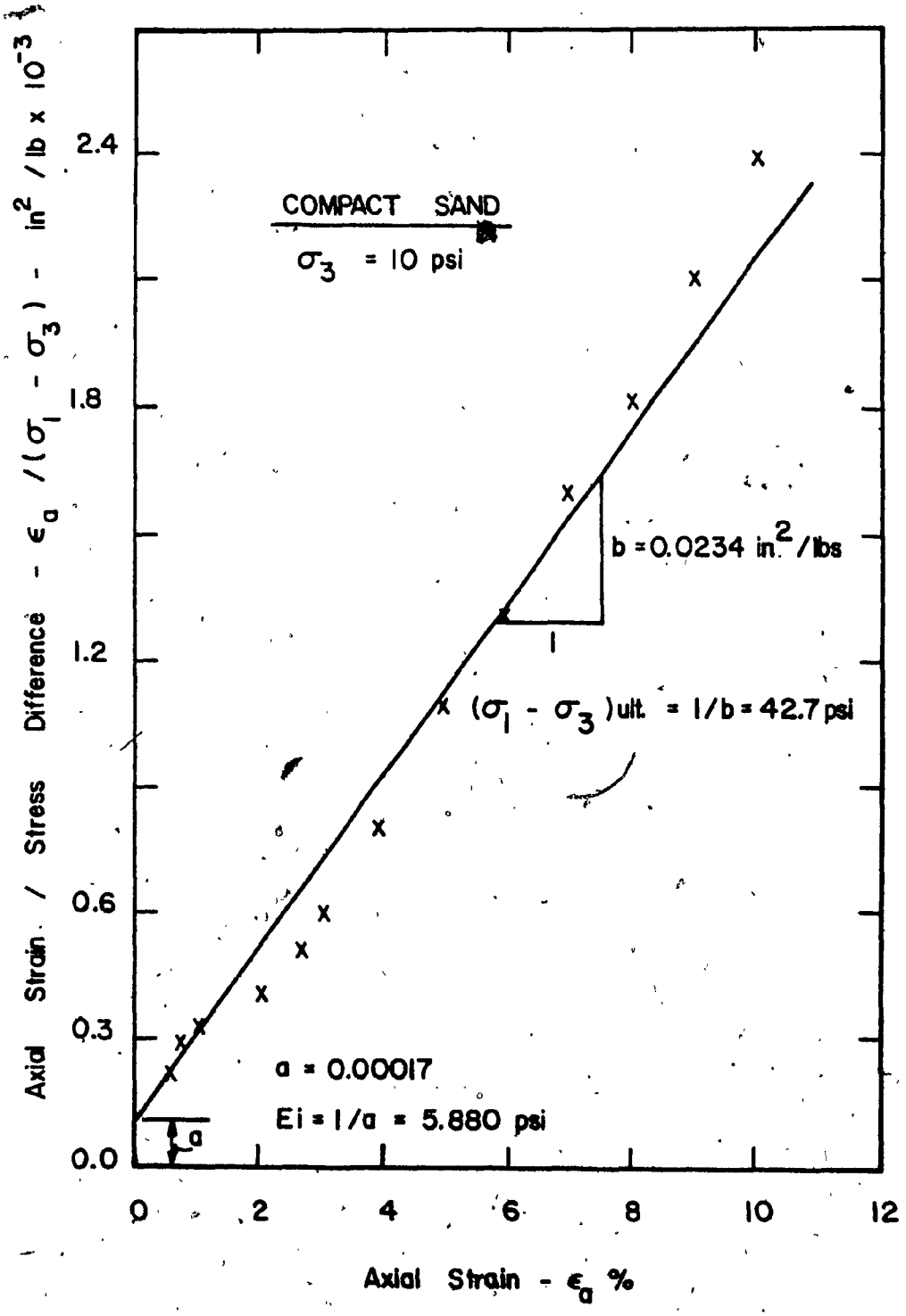

FIG. 5.2b TRANSFORMED STRESS - STRAIN CURVE

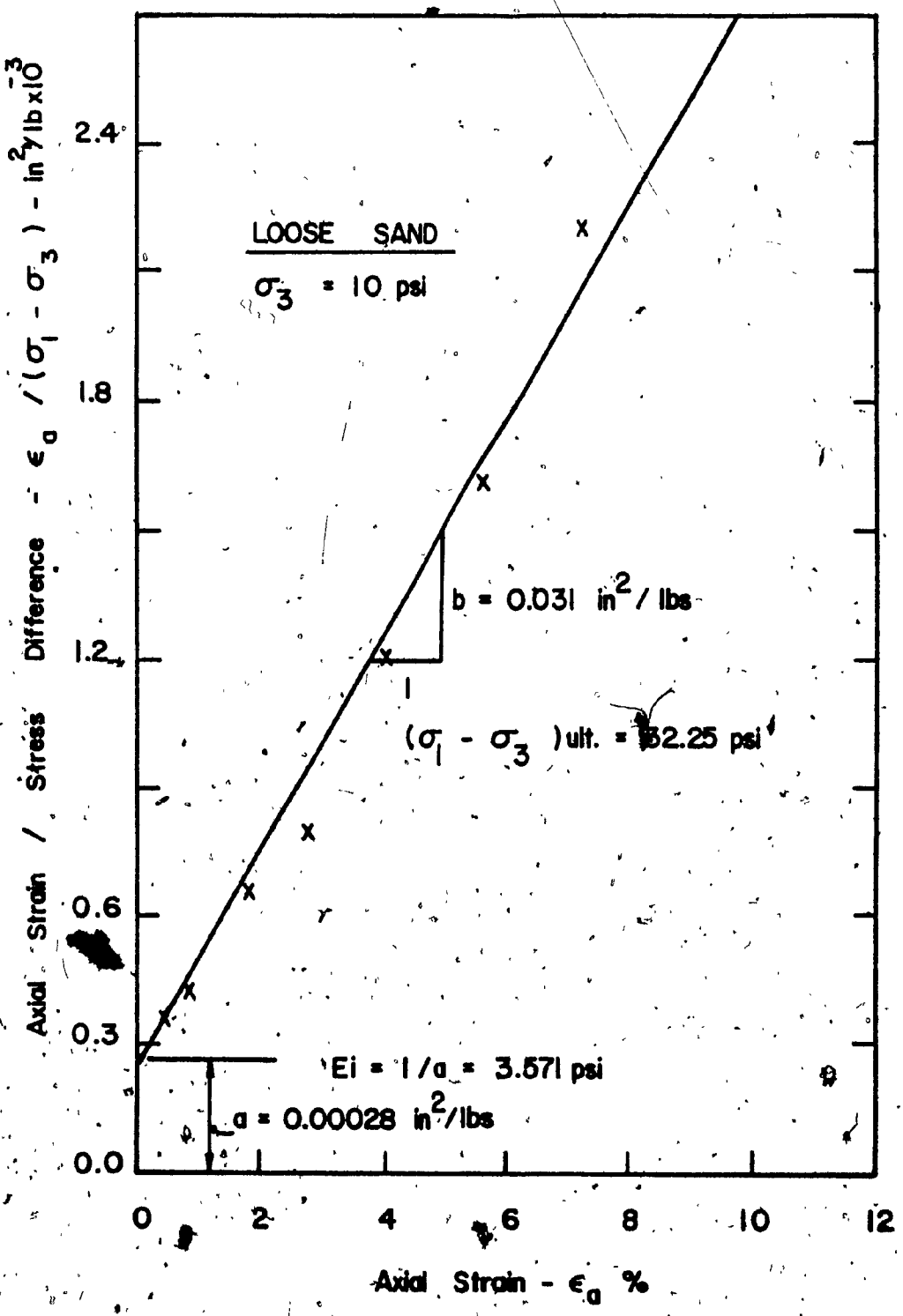

FIG. 5.2c TRANSFORMED STRESS - STRAIN CURVE

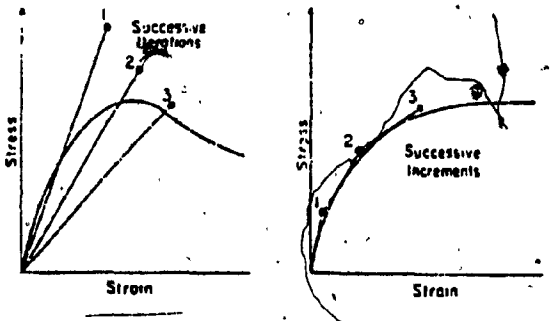

Fig. 5.3 Techniques for approximating nonlinear stress-strain behavior.

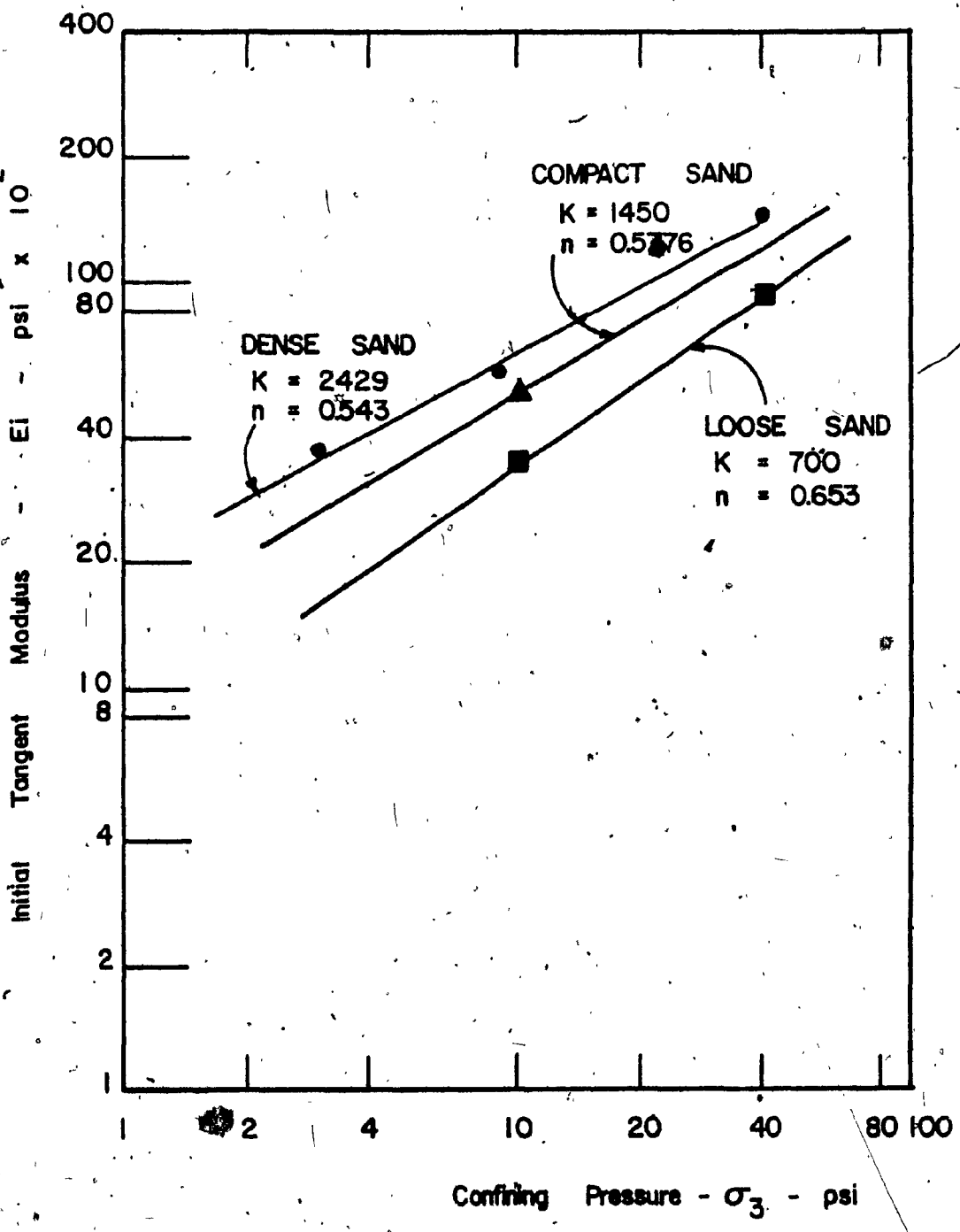

FIG. 5.4 VARIATIONS OF INITIAL TANGENT MODULUS WITH CONFINING PRESSURE FOR THE PLANE STRAIN CONDITION

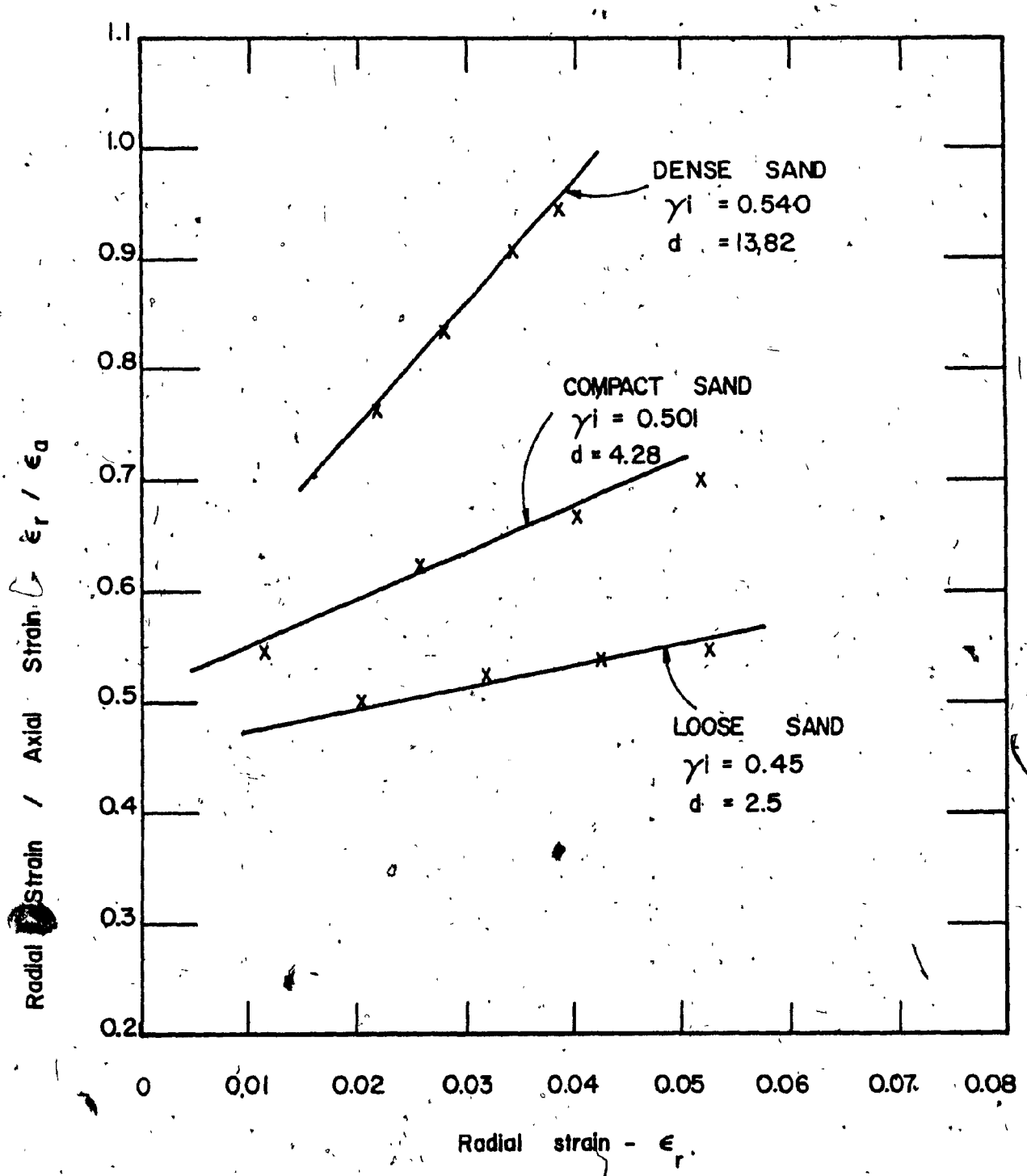

FIG. 5.5 VARIATION OF RADIAL / AXIAL STRAIN WITH RADIAL STRAIN

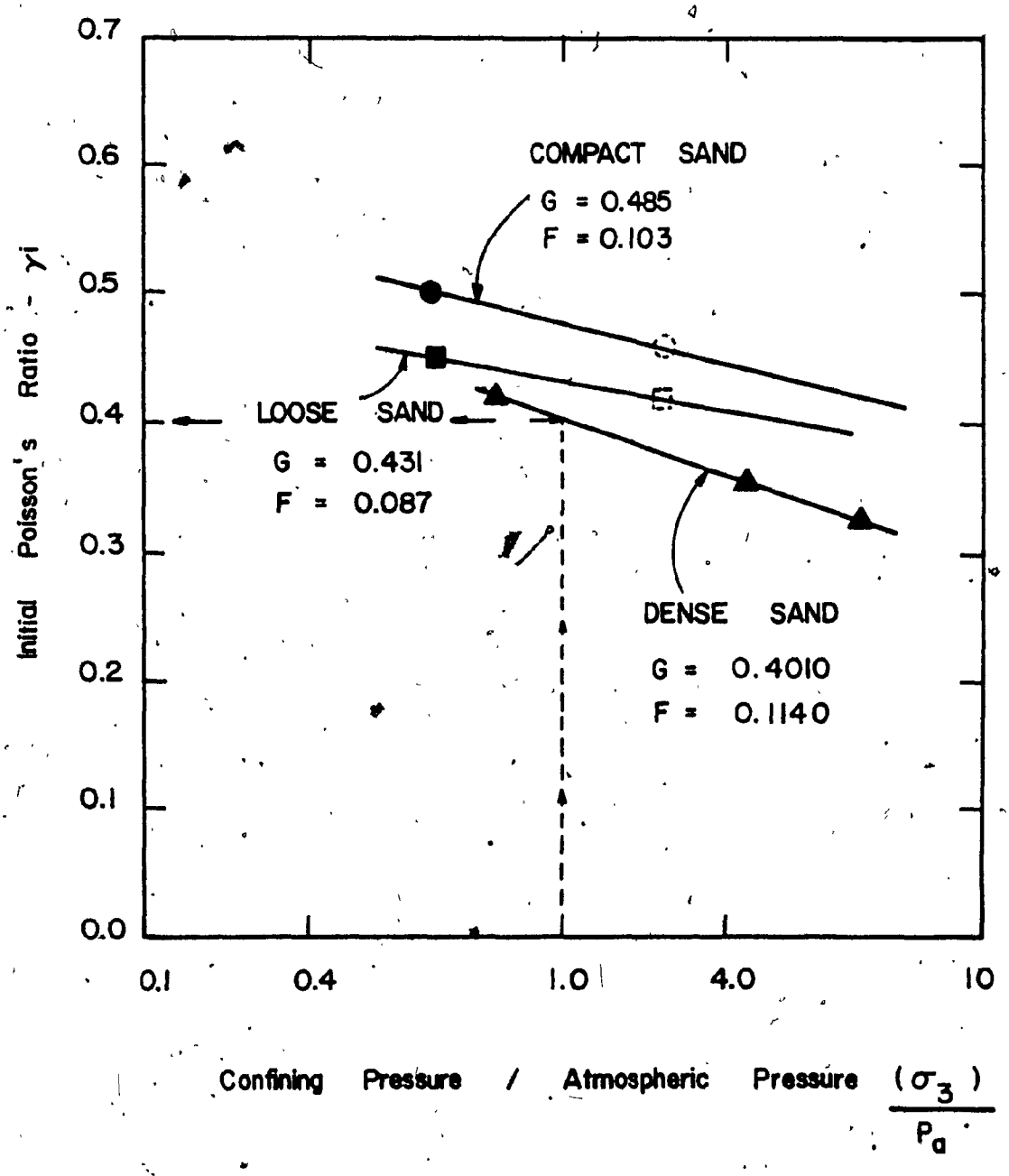

FIG. 5.6 VARIATION OF INITIAL POISSON'S RATIO WITH CONFINING PRESSURE / ATMOSPHERIC PRESSURE

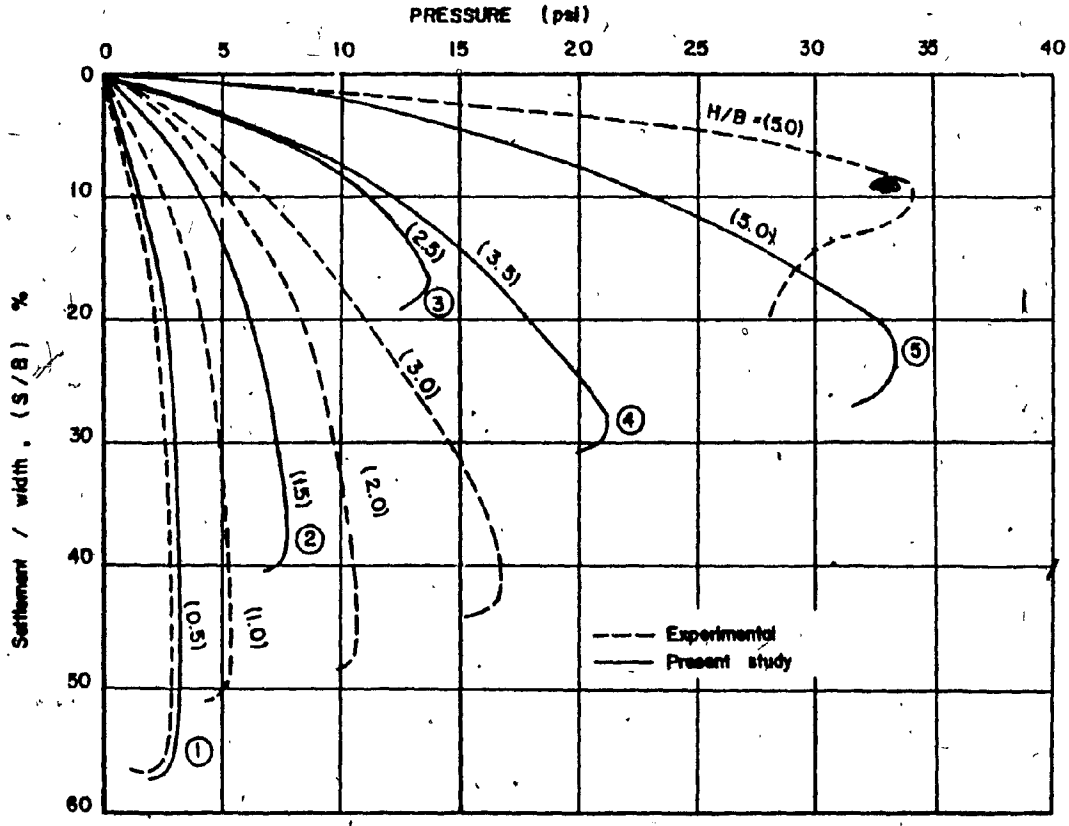

FIG. 5.7 LOAD SETTLEMENT CURVES - SURFACE STRIP FOOTING ON DENSE SAND OVERLYING LOOSE SAND (GROUP A')

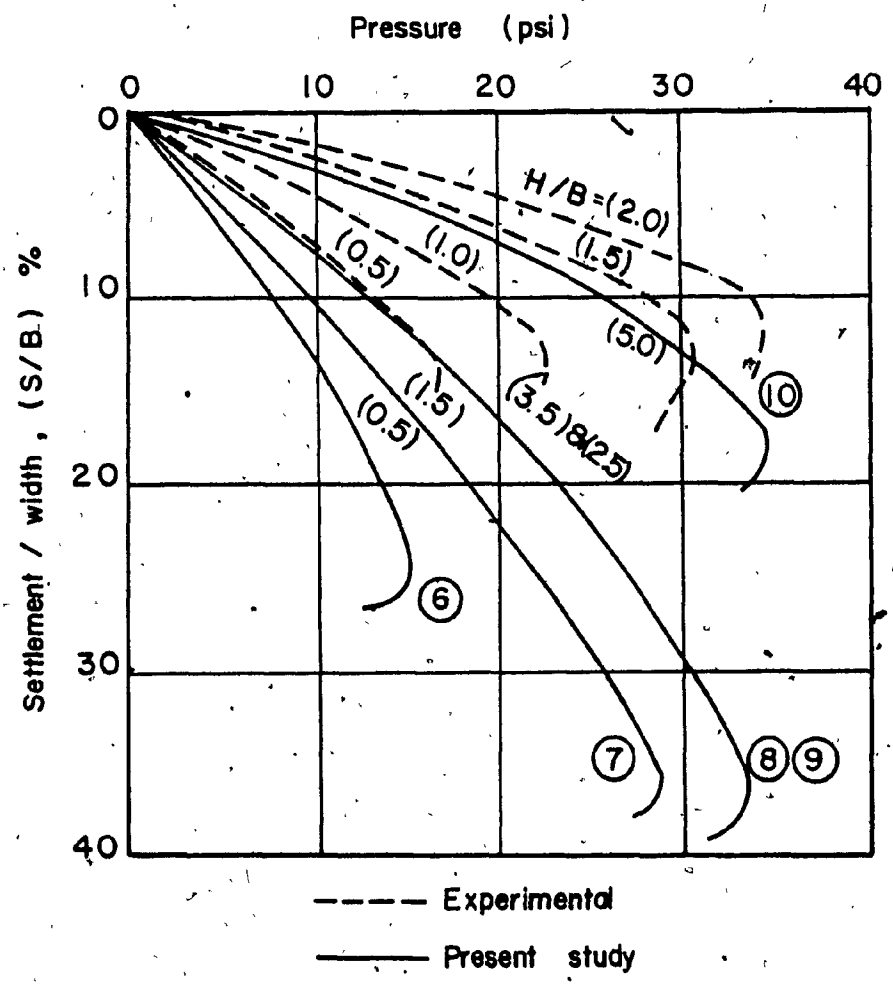

FIG. 5.8. LOAD SETTLEMENT CURVES - SURFACE STRIP FOOTING ON DENSE SAND OVERLYING COMPACT SAND (GROUP B)

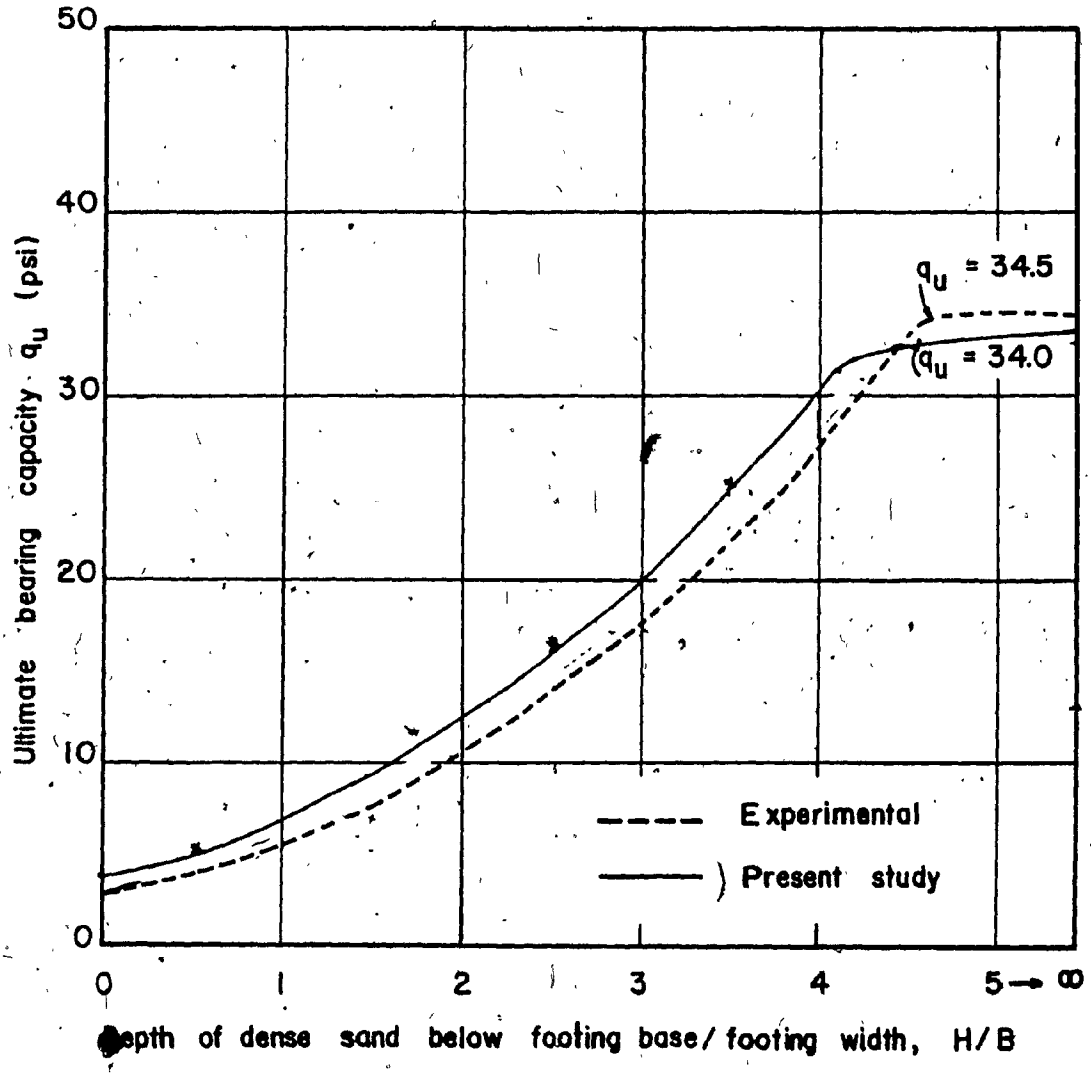

FIG. 5.9 q_u VERSUS H/B RATIO FOR SURFACE STRIP FOOTING ON DENSE SAND OVERLYING LOOSE SAND.

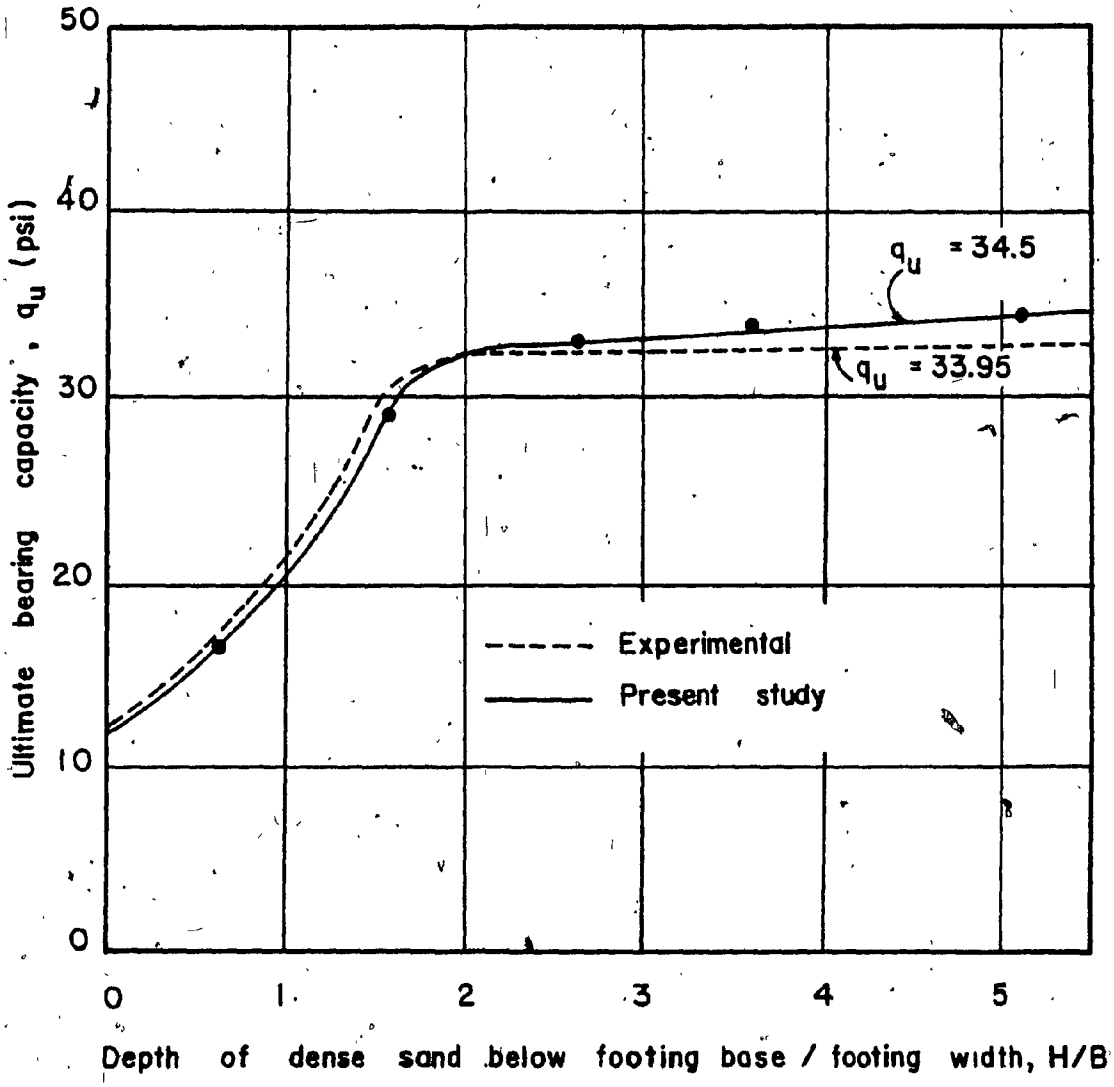

FIG. 5.10 q_u VERSUS H/B RATIO FOR SURFACE STRIP FOOTING ON DENSE SAND OVERLYING COMPACT SAND

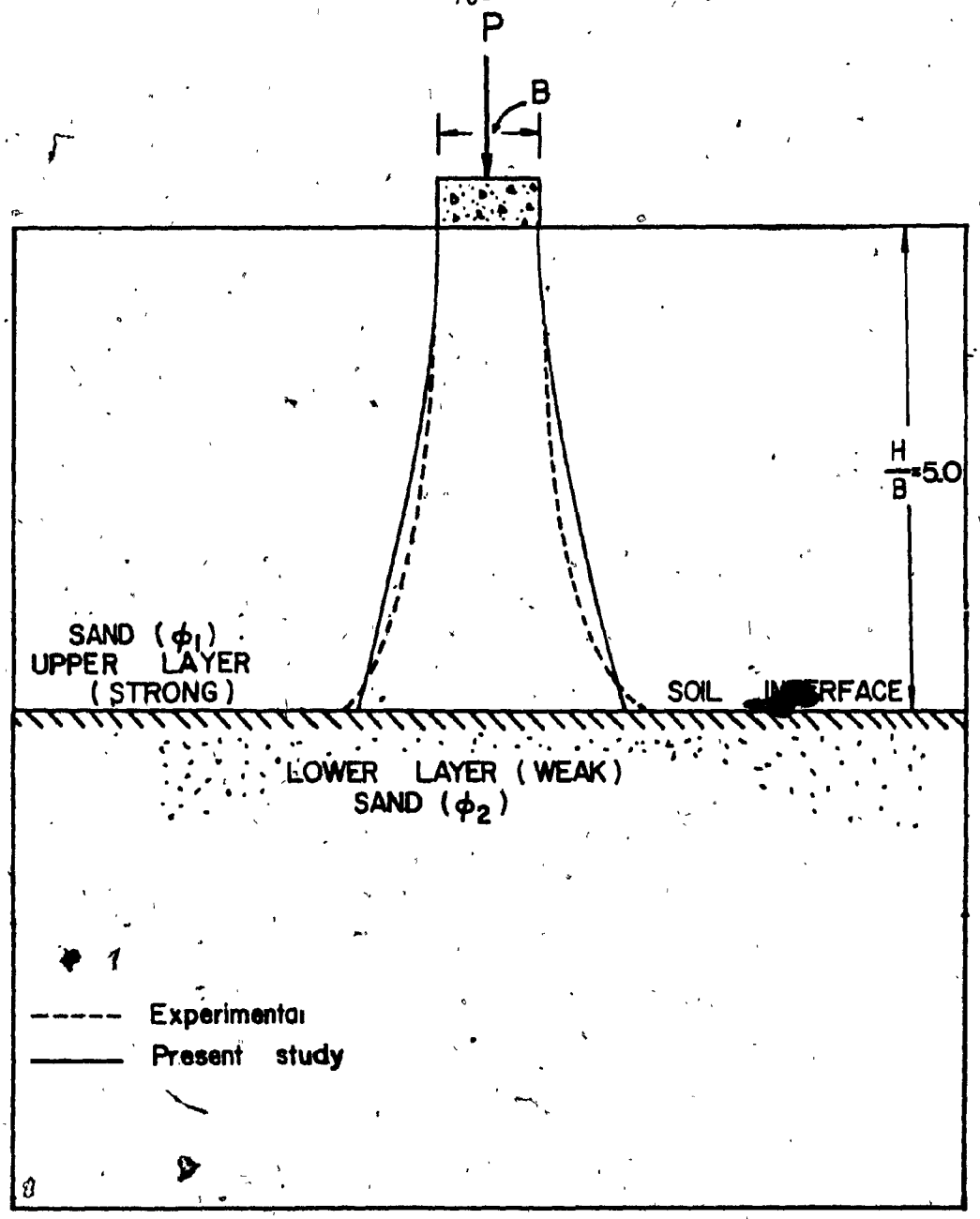

FIG. 5.11 DISTRIBUTION OF THE LOCAL ANGLE OF SHEARING RESISTANCE OF THE FAILURE PLANE

STRIP FOOTING ON A STRONG LAYER OF SAND OVERLYING A WEAK LAYER OF SAND

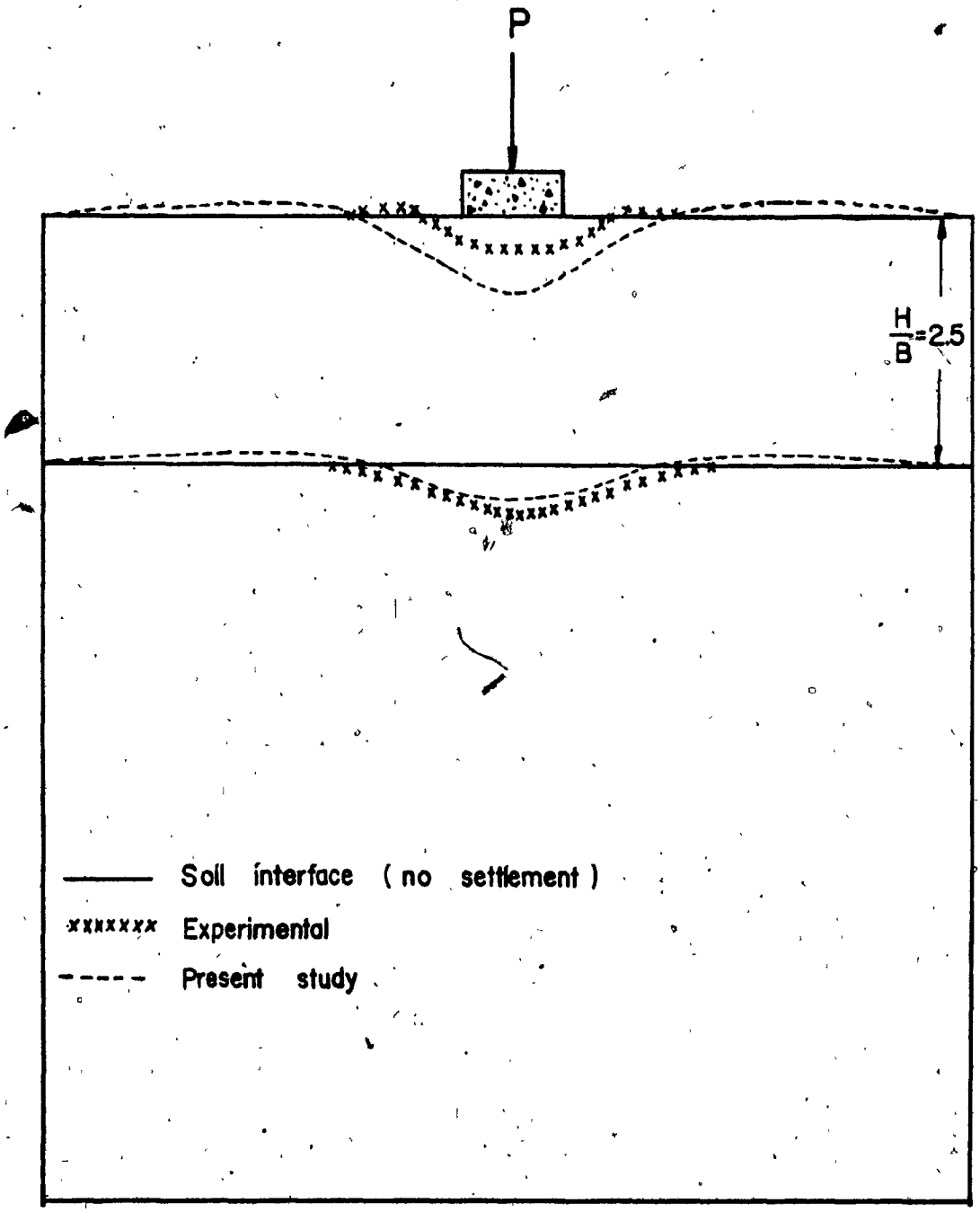

FIG. 5.12 LAYER SETTLEMENT OF STRIP FOOTING UNDER VERTICAL LOAD IN DENSE SAND OVERLYING LOOSE SAND

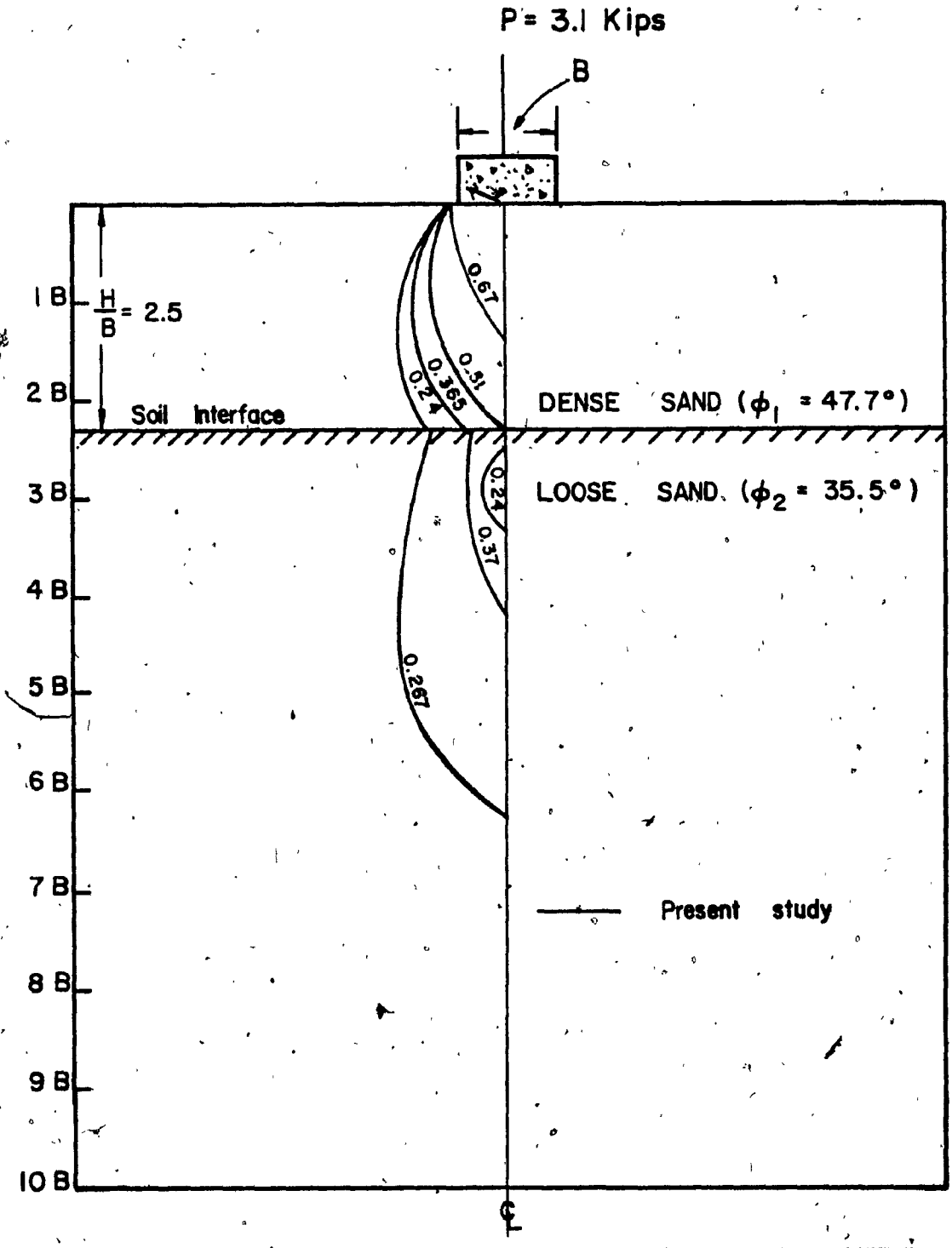

FIG. 5.13 PRESSURE ISOBARS BELOW A STRIP FOOTING BASED ON THE PRESENT ANALYSIS FOR q_o = 10.8 psi

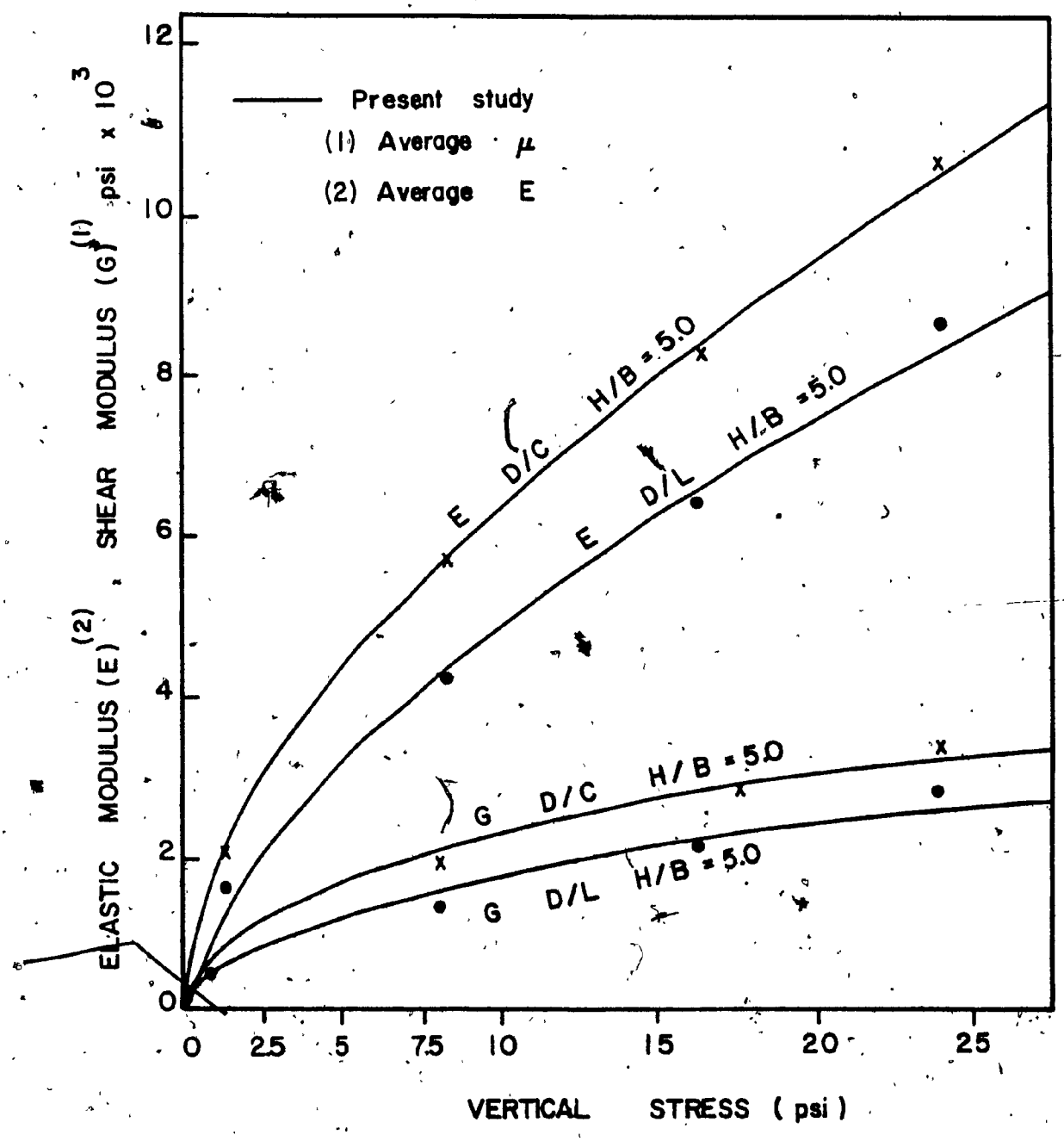

FIG. 5.14 BEHAVIOR OF THE SAND DURING TWO-DIMENSIONAL COMPRESSION. ELASTIC MODULUS AND SHEAR MODULUS FROM ZERO PSI TO INDICATE STRESS.

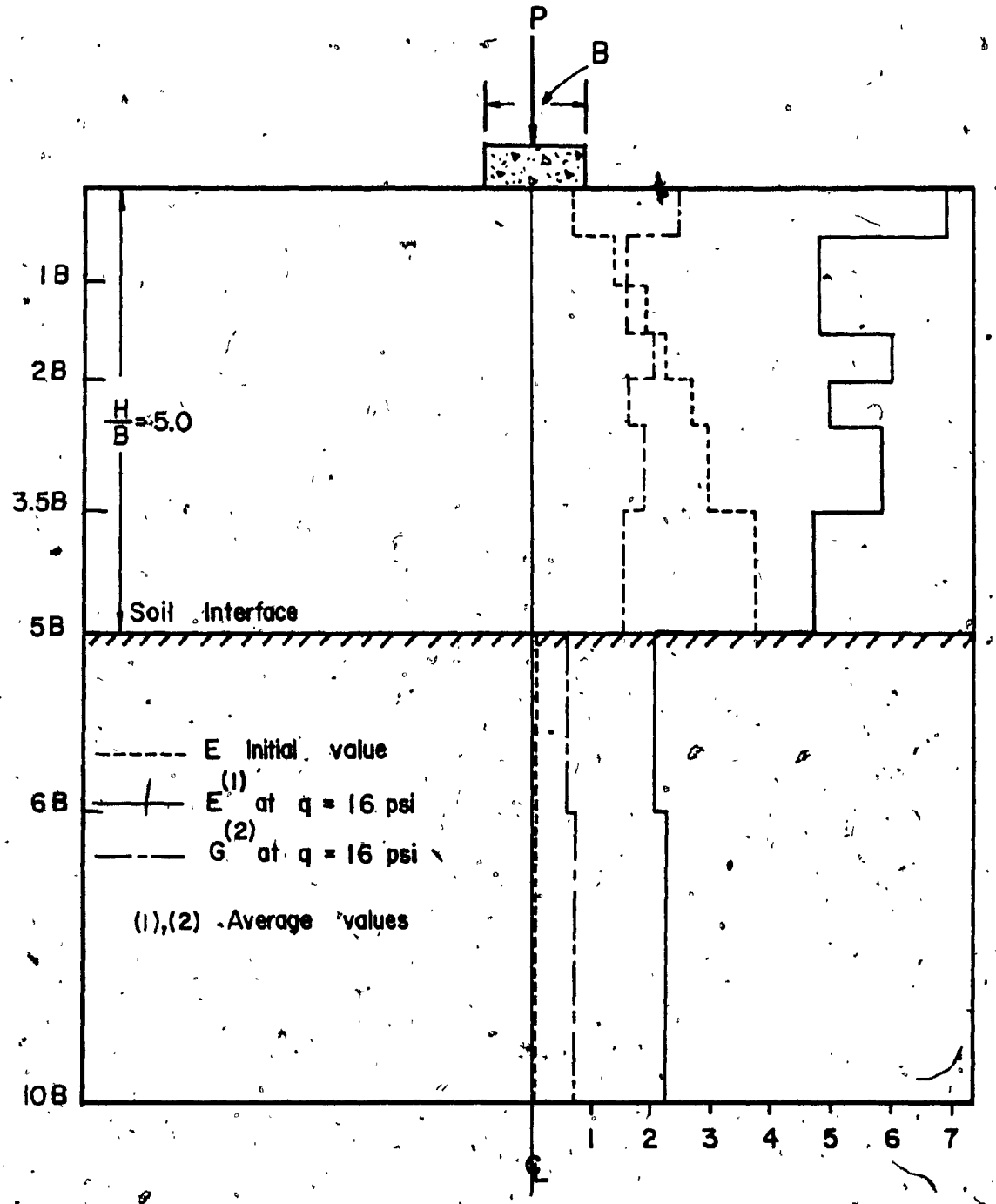

FIG. 5.15 VARIATION OF ELASTIC MODULUS (E) AND SHEAR MODULUS (G) DIRECTLY BELOW A STRIP FOOTING WITH DEPTH, FOR D/L SAND.

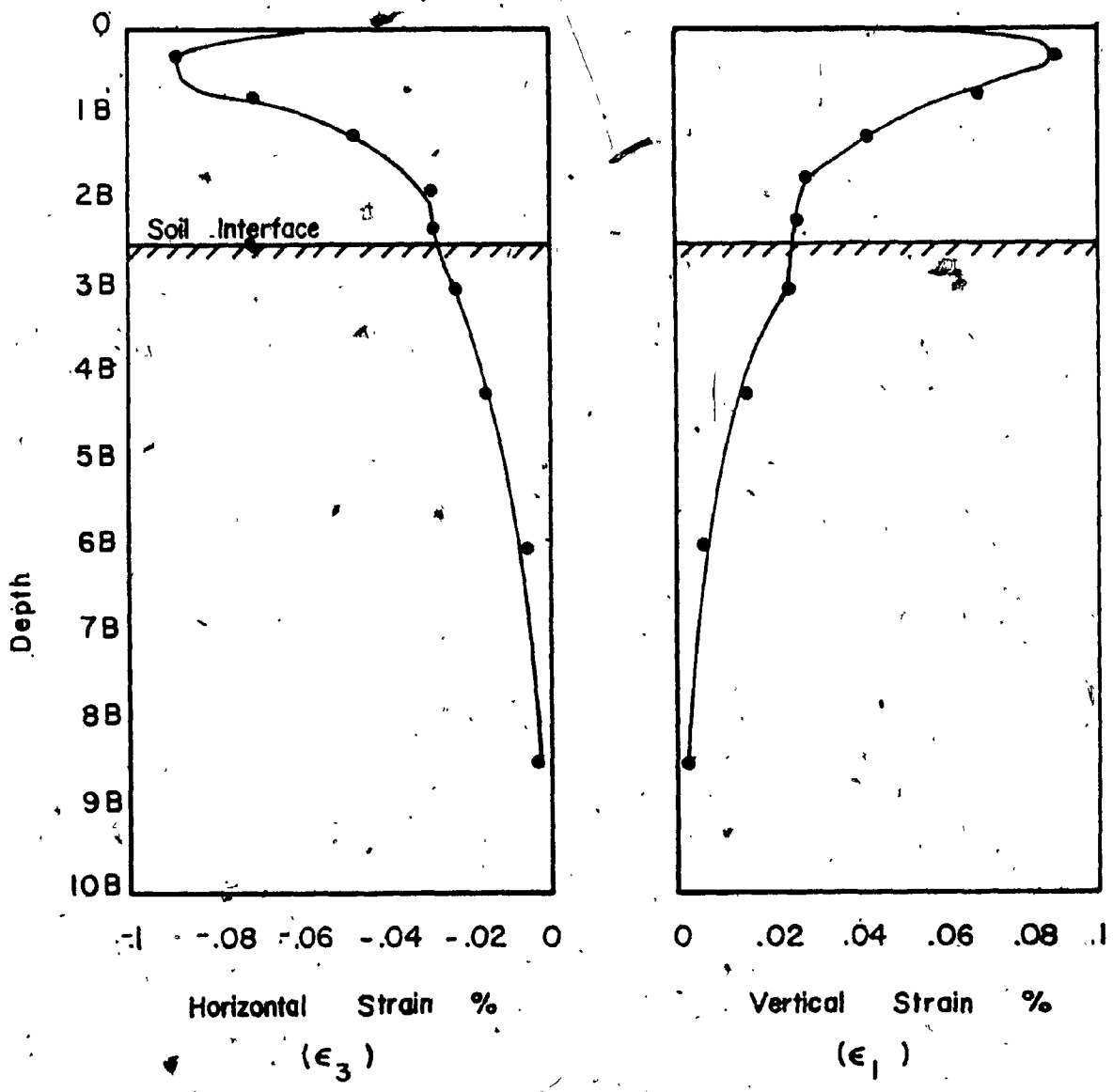

FIG. 5.16 FINITE - ELEMENT COMPUTED STRAINS ASSUMING NON - LINEAR SOIL BEHAVIOR

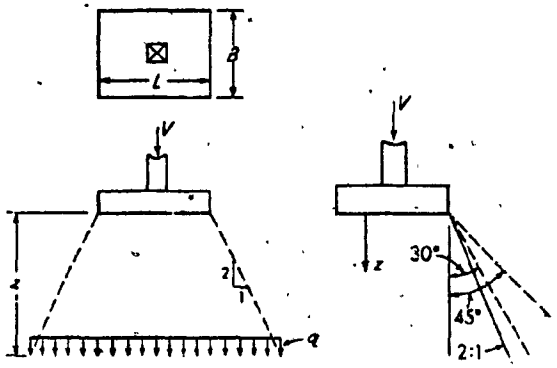

Fig.5.17 Approximate methods of evaluating stress increase in the soil at a depth z beneath the footing.

REFERENCES

1. Bowles, J.E., (1977). "Foundation Analysis and Design". New York: Mc Graw-Hill Publishing Co.

2. Button, S.J. 1953. The Bearing capacity of Footings on a two Layer Cohesive Subsoil. Proc. Third Int. Conf. Soil Mech. Found. Eng. Zurich, Switz, 1, pp. 332-335.

3. Chiyyarath V and C. Reese. "Finite-element Method for Problems in Soil Mechanics." Journal of the Soil Mechanics and Foundation Division - Proceedings of the American Society of Civil Engineers." SM2 March, 1968.

4. Clough, R.W. "The Finite-Element Method in Plane Stress Analysis". Proceedings of the 2nd ASCE Conference on Electronic Computation. Pittsburgh, 1960.

5. Desai, C.S. and Reese L. 1970a. "Ultimate capacity of circular Footings on Layered Soils. J. Indian Nat. Soc., Soil Mech. Found. Eng. 96 (1) pp. 41-50.

6. Duncan, J.M., and Chang, C.Y. (1970) "Nonlinear Analysis of Stress and Strains in Soils"., Journal of the Soil Mechanics and Foundations division, ASCE, Vol. 96 No.SM5, Sept., pp.1629-1653.

7. Hanna, A.M., (1978), "Bearing Capacity of Footing Under Vertical and inclined loads on Layered Soils. Ph. D. Thesis, Nova Scotia Technical College, Halifax, N.S.

8. Hrennikoff A. "Solution of Problems of Elasticity by the Framework Method", Journal of Applied Mechanics, ASME Vol. 63, December 1941, pp. A-169 to A-175.

9. Kulhawy, F.H., and Duncan, J.M., "Nonlinear Finite Element Analysis of Stresses and Movements in Oroville Dam," Report No. TE 70-2. Office of Research Services, University of California, Berkeley, 1970.

10. Kondner, R.L., (1963), "Hyperbolic Stress-Strain Response: Cohesive Soils", Journal of the Soil Mechanics and Foundations Division, ASCE, Vol. 89, No. SMI, pp. 115-143.

11. Lebeque, Yves, "Fondations Superficielles reposant sur un milieu Bi-couche. Comptes rendus des recherches effectuées par les organismes de l'Union Technique Interfédérale du Bâtiment et des Travaux Publics". Annales I.T.B.T.P., juin 1966 No.222, p.699 et juin 1967 No. 234 p. 803.

12. McCormick, C.W. "Plane Stress Analysis" Proceedings of the 3rd ASCE Conference on Electronic Computation, Boulder Colo. Journal of the Structural Division, ASCE Vol. 89, No. ST 4, August 1963, Part I pp. 39-54.

13. McHenry D. "A Lattice Analogy for the Solution of Stress problems". Journal of the Institution of Civil Engineers, Vol. 21-22 No.2 Paper No.5350, 1943-1944 December 1943, London pp. 59-82.

14. Meyerhof G.G. and Hanna, A.M., (1978), "Ultimate Bearing capacity of Foundations on Layered Soils Under Inclined loads", Canadian Goetechnical Journal, Volume 15, No.4, pp. 565-572.

15. Meyerhof, G.G., and Brown, J. 1967, Discussion on Bearing capacity of Layered Clay by Sivareddy, A., and Srinivasan, R., J.J. Soil. Mech. Found. Eng. Volume 93 (5) pp. 361-362.

16. Meyerhof, G.G. "Ultimate Bearing Capacity of Footings on Sand Layer Overlying Clay". Canadian Goetechnical Journal Volume II Number 2 May 1974.

17. Meyerhof, G.G., 1965, "Shallow Foundations", Jl Soil Mech. Found. Eng., ASCE, Vol. 95, No.SM2, p.21.

18. Meyerhof, G.G. and Valsangkar, A.J. 1977, "Bearing Capacity of Piles in Layered Soils", Proc. 9th Int. Conf. on Soil Mech., Vol.2, Tokyo Japan.

19. Myslivec, A., 1971, "Bearing Capacity of Layered Subsoil", Proc. 4th Budapest Conference on Soil Mechanics and Foundation Engineering p.677.

20. Purushothamaraj P. and Rao "Bearing Capacity of Strip Footings in two Layered Cohesive-friction Soils". Can. Geotech. Journal 11, 32 1974.

21. Reddy, A.S. and R.J. Srinivasan (1967) "Bearing Capacity of Footings on Layered Clays, JSMFD, ASCE, Vol. 93, SM 2, March pp.83-99.

22. Terzaghi, K., 1943, "Theoretical Soil Mechanics", John Wiley and Sons, New York.

23. Terzaghi, K. and Peck, R.B., 1967, "Soil Mechanics in Engineering Practice", 2nd ed., John Wiley and Sons, New York.

24. Wilson Edward L. "Structural Analysis of Axisymmetric Solids" Journal of the American Institute of Aeronautics and Astronautics. Dec. 1965.

25. Yamaguchi, H. "Practical Formula of Bearing Value for two Layered Ground. Proc. Second Asian Reg. Conf. Soil Mech. Japan, pp. 52-62 1963 .